BSGF
Earth Sciences Bulletin

Special Issue Messinian Crisis, Jean-Pierre Suc and Jean-Loup Rubino (Guest Editors)

Available online at:
www.bsgf.fr

OPEN ACCESS

Salt tectonics evolution in the Provençal Basin, Western Mediterranean Sea

Massimo Bellucci[1,2,*], Estelle Leroux[1], Daniel Aslanian[1], Maryline Moulin[1], Romain Pellen[1] and Marina Rabineau[1]

[1] Geo-Ocean, Univ Brest, CNRS, Ifremer, UMR6538, 29280 Plouzané, France
[2] University of Trieste, Department of Mathematics and Geosciences, Via Weiss 1, 34128, Trieste, Italy

Abstract – The Messinian Salt Giant in the Provençal Basin represents a good example to study salt tectonics: salt deposition occurred throughout the basin well after basin opening, with a tectonic context stable since ~16 Ma, in a closed system. Also, the youth of salt tectonics has led to less mature structures and an evolutionary history that is easier to decipher than in older salt-bearing margins. We conducted an analysis of the chronology of salt deformation, from its deposition to the present-day, thanks to the basin-wide correlation of the Late Miocene and Pliocene-Pleistocene stratigraphic markers. The large seismic dataset provided detailed analysis of the causes and timing of salt deformation at a regional level. The salt tectonics started relatively early, during the Messinian Upper Unit (UU) deposition (phase 1) in the deepest part of the basin. From the Pliocene to the present-day, salt movement is divided into two more main phases (phases 2 and 3), the first of small intensity, occurred during the Pliocene and the second, more intense, during the Pleistocene. The geometric relationship between salt tectonics and crustal nature domains has revealed, regardless of the timing deformation phases, a more rapid and intense salt deformation above the proto-oceanic crust domain than in the continental or transitional crust domain. This observation, remaining unexplained, emphasizes the role of the influence of crustal nature, associated thermal regime and fluid circulation system on salt tectonics.

Keywords: Salt tectonics / Messinian salinity Crisis / Gulf of Lion / Provençal basin / Western Mediterranean / Crustal segmentation

Résumé – Évolution de la tectonique salifère dans le Bassin Provençal, Mer Méditerranée occidentale. Le Géant Salifère Messinien dans le Bassin Provençal représente un exemple approprié pour étudier la tectonique salifère : le sel s'est déposé dans tout le bassin bien après le rifting, dans un contexte tectonique stable depuis environ 16 millions d'années et dans un système fermé. De plus, l'âge de la tectonique salifère a conduit à des structures moins complexes et à une histoire évolutive plus facile à déchiffrer que dans les marges salifères plus anciennes. Nous avons mené une analyse de la chronologie de la déformation du sel, depuis son dépôt jusqu'à nos jours, grâce à la corrélation à l'échelle du bassin des marqueurs stratigraphiques du Miocène supérieur et du Pliocène-Pléistocène. Le vaste ensemble de données sismiques a permis une analyse détaillée des causes et du timing de la déformation du sel à un niveau régional. La tectonique salifère a commencé relativement tôt, pendant le dépôt de l'Unité Supérieure Messinienne (UU) (phase 1) dans la partie la plus profonde du bassin. Du Pliocène jusqu'à nos jours, la déformation du sel est divisée en deux phases principales supplémentaires (phases 2 et 3), la première de faible intensité, survenue pendant le Pliocène et la seconde, plus intense, pendant le Pléistocène. La relation géométrique entre la tectonique salifère et les domaines de nature crustale a révélé, indépendamment des phases de déformation temporelle : une déformation du sel plus rapide et plus intense au-dessus du domaine de la croûte proto-océanique que dans le domaine de la croûte continentale ou transitionnelle. Cette observation, qui reste inexpliquée, souligne le rôle de l'influence de la nature crustale, du régime thermique associé et du système de circulation des fluides sur la tectonique salifère.

Mots clés : Tectonique Salifère / Crise de Salinité Messinienne / Golfe du Lion / Bassin Provençal / Méditerranée Occidentale / Segmentation crustale

*e-mail: mass.bellucci@gmail.com

1 Introduction

The study of salt tectonics has been of fundamental importance in oil exploration since its inception. Salt is considered impermeable to fluids and gases, making it an excellent seal. Furthermore, given its mobility, it deforms at geological time scales, thus forming traps and influencing the distribution of reservoirs. More recently, the characteristics of salt are in the spotlight regarding subsurface storage. Storage can be located directly within the salt or in sedimentary traps created by its deformation (*e.g.* Duffy *et al.*, 2022). Another significant property of salt is its high thermal conductivity (Mello *et al.*, 1995): salt acts as a heat pump, with obvious implications in geothermal energy and oil window productivity. Also, temperature influences salt tectonics: an increase in temperature leads to a decrease in viscosity and thus faster deformation (Carter *et al.*, 1993). The thermal regime, jointly with the most important factors triggering salt tectonics, such as salt thickness variation, sedimentation, basin tilt, salt purity, tectonics, could potentially have a strong influence on salt mobility.

In the Mediterranean Sea, salt was deposited during the Messinian Salinity Crisis (MSC) in the deep parts of aborted basins, at a time when the drop in sea level (or beneath a deep-water saline basin, *e.g.* Christeleit *et al.*, 2015) caused thick evaporites deposition within a relatively short time ($\sim$0.64 Ma) (between 5.96 and 5.33 Ma) (Gautier *et al.*, 1994). In all the Mediterranean Sea, salt is generally deposited above a marine sedimentary sequence and crust that spans from continental, to transitional and oceanic.

In this paper, we focus our study on the Provençal Basin, located in the Western Mediterranean Sea, because of a considerable amount of data (seismic and well data) and in-depth knowledge of the sedimentary column and deep crustal segmentation from previous studies. The youth of the salt layer and the stable tectonic setting that followed its deposition has led to less mature salt tectonic structures and an evolutionary history that is easier to decipher than in other margins around the world (*e.g.* Gulf of Mexico, Brazilian or Angola basins). The discussion around salt morphology and tectonics in this area began with the works of Pautot *et al.*, 1984), followed by Le Cann 1987), Gorini 1993), Gaullier 1993), Dos Reis *et al.*, 2005, Dos Reis *et al.*, 2008,), Gaullier *et al.*, 2008) and Mianaekere *et al.*, 2020a, 2020b). Similar to other worldwide salt passive margins (*e.g.* Cobbold and Szatmari, 1991; Demercian *et al.*, 1993; Letouzey *et al.*, 1995; Vendeville, 2005; Jackson and Hudec, 2017), the authors (Gaullier, 1993; Gorini, 1993; Dos Reis *et al.*, 2005;) describe three salt kinematic domains from the lower slope to the deep basin: (i) a proximal *extensional* domain, (ii) a mid-slope *translation* domain and (iii) a distal *shortening* domain. The salt structures characterising these domains are interpreted as the result of thin-skinned tectonics controlled by sedimentary spreading and gravity gliding (Dos Reis *et al.*, 2008, Mianaekere *et al.*, 2020a, 2020b; Granado *et al.*, 2016; Obone-Zue-Obame *et al.*, 2011; Geletti *et al.*, 2014; Dal Cin *et al.*, 2016). Other hypotheses include thick-skinned tectonics (Pautot *et al.*, 1984; Le Cann, 1987; Maillard *et al.*, 2003) with a significant role of the basin-scale shape of the salt layer (Gaullier *et al.*, 2008). Several authors claim that salt tectonics started after the deposition of the Messinian Upper Unit (UU) during the Lower Pliocene, due to basinward tilting subsidence and/or sedimentary thickness (*e.g.* Dos Reis *et al.*, 2005). Gaullier *et al.*, 2018) described for the first time an early salt movement in the deep basin concomitant with the deposition of the UU (last phase of the MSC), recently confirmed by Bellucci *et al.*, 2021a). Nevertheless, the lack of accurate dating of the Pliocene-Pleistocene sequences has so far precluded a more in-depth discussion of the timing and causes of deformation. In this work, through detailed analysis of seismic geometries and deformation, we present a detailed study of salt tectonics phases and timing in the Provençal Basin.

2 Regional setting and MSC stratigraphy

The Provençal Basin (Fig. 1) is a young passive margin formed after the counter-clockwise rotation of the Corso-Sardinian blocks started in the Late Eocene (Auzende *et al.*, 1973; Olivet, 1996). A relatively short-lived rifting phase ($\sim$9 Ma; Réhault *et al.*, 1984; Gattacceca *et al.*, 2007) was followed by oceanic spreading which led to the formation of a thin atypical oceanic crust in the deep basin (Afilhado *et al.*, 2015; Moulin *et al.*, 2015; Bache *et al.*, 2010). Since $\sim$16 Ma (Leroux *et al.*, 2019), the Provençal Basin has not been affected by any major tectonic movement. Describing the sedimentary markers and their paleobathymetric significance, Rabineau *et al.*, 2014) observed a purely vertical subsidence in the Gulf of Lion deep basin and tilting in the continental domain, subsequently confirmed by an extensive 3D regional analysis and numerical stratigraphic modelling by Leroux *et al.*, 2015a, 2015b). On the shelf and slope, the subsidence consists of seaward tilting while the deep basin subsides vertically (Fig. 2). The limit between tilting and purely vertical subsidence coincides with the limit between thinned continental and exhumed lower continental crust (Fig. 1A) constrained by wide-angle refraction data (Moulin *et al.*, 2015) and deep reflection seismic lines (Bache *et al.*, 2010).

The stratigraphy of the Provençal Basin has been investigated at various levels, from the syn-rift to Pleistocene sequences (*e.g.* Gorini, 1993; Lofi *et al.*, 2005; Droz *et al.*, 2020; Rabineau *et al.*, 2006; Leroux *et al.*, 2017). The short-term Messinian Salinity Crisis (MSC; Hsü *et al.*, 1973) event ($\sim$5.96–5.33 Ma, Gautier *et al.*, 1994) strongly impacted the stratigraphy of the whole Mediterranean region. Restriction of the connection between the Atlantic Ocean and the Mediterranean Sea (*e.g.* Benson *et al.*, 1991) led to the deposition of thick evaporites, including around 0.8–1 km of halite, also called Mobile Unit (MU) (Lofi *et al.*, 2011, Lofi *et al.*, 2018). In the Provençal Basin, salt was deposited in a stable tectonic context, above a thick ($\sim$2 km) marine sedimentary sequence (Fig. 2).

In this work, we use the term "Salt" for the MU described in Lofi *et al.*, 2011, Lofi *et al.*, 2018. We further consider an undetermined "pre-salt" sequence composed of syn- and post-rift sedimentation of Oligocene-Miocene age (Fig. 3) including the Messinian Lower Unit (LU) deposited before the salt (*i.e.* LU from Lofi *et al.*, 2011 and LU1 and LU0 from Bache *et al.*, 2009) (Fig. 5). LU sequence is considered as the expression of the first phase of the MSC, composed of detrital deposits possibly intercalated with evaporites. The thick pre-salt mega-sequence onlaps the acoustic basement, infilling earlier
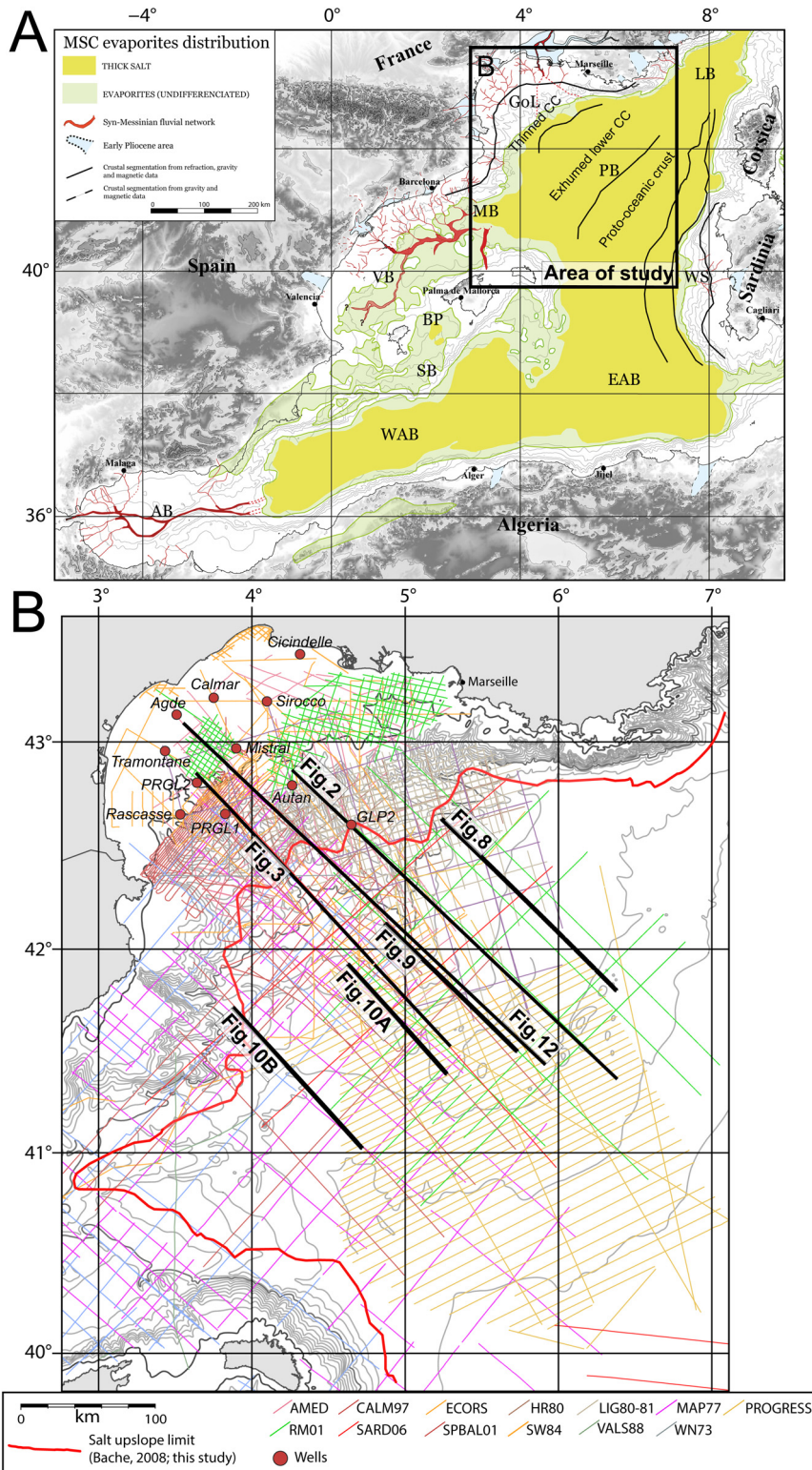
Fig. 1. (A) Extension map of the MSC evaporites distribution in the Western Mediterranean Sea showing the frame of the study area (modified after Pellen *et al.*, 2019). Labels: AB: Alboran Basin; BP: Balearic Promontory; EAB: Eastern Algerian Basin; GoL: Gulf of Lion margin; LB: Ligurian Basin; MB: Menorca Basin; PB: Provençal Basin; SB: south Balearic margin; VB: Valencia Basin; WAB: Western Algerian Basin; WS: Western Sardinian margin. Crustal segmentation is taken from Moulin *et al.*, 2015, Afilhado *et al.*, 2015 and Leroux *et al.*, 2019. B Reflection seismic data used for this study. Borehole positions in red circles are taken from Leroux *et al.*, 2017 while red line indicates the upslope Messinian salt (Mobile Unit) limit, after Bache *et al.*, 2009 and this study.

Fig. 1. *(A) Carte d'extension de la distribution des évaporites de la CSM (Méditerranée Occidentale) localisant la zone d'étude (modifiée d'après Pellen* et al*., 2019). (B) Données sismiques de réflexion utilisées pour cette étude.*
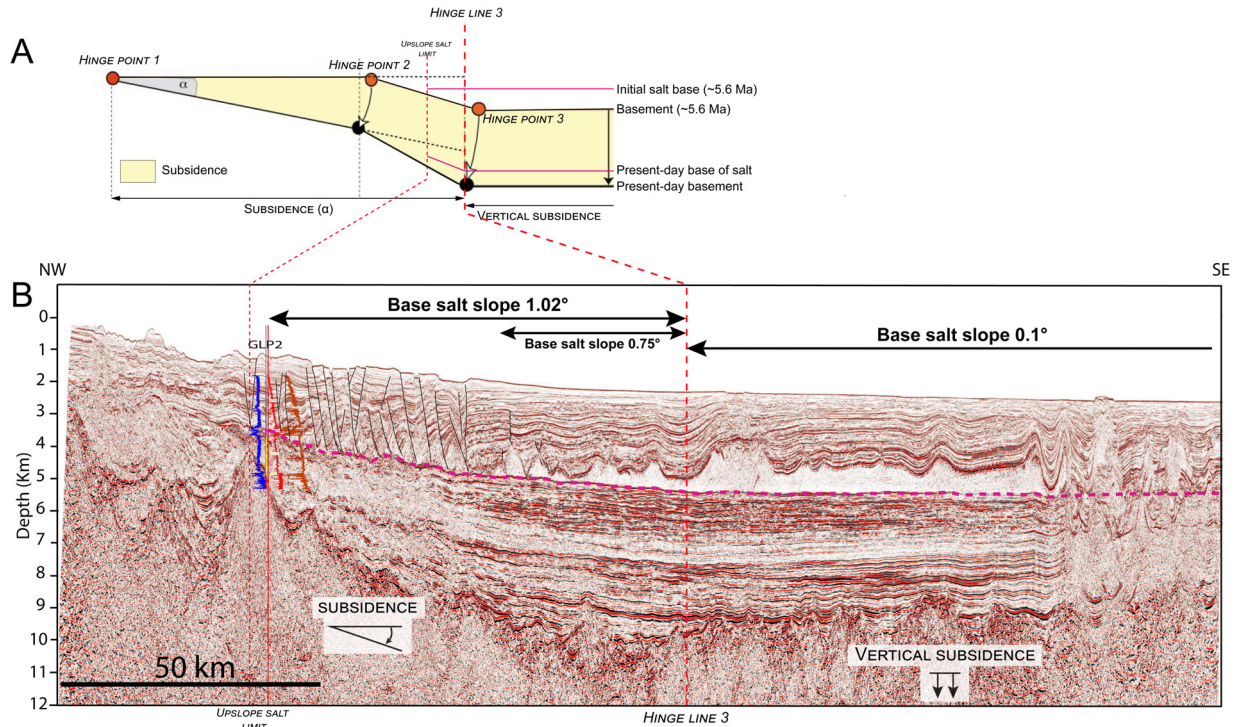
Fig. 2. (A) Sketch illustrating how has been analysed the subsidence pattern of the Provencal Basin (modified after Rabineau, 2001 and Leroux, 2012). Hinge line 3 marks the boundary between a tilting and purely vertical subsidence. Dotted black lines highlight the slope changing basinward the hinge points. Note the increasing slope history on the margin given by subsidence while the deep basin subsides purely vertically. B) Seismic profile (in depth, km) (TGS-Nopec) crossing perpendicularly the Provençal Basin (location in Fig. 1) showing the base of salt slope values (dashed purple line) in the lower slope and deep basin. The profile is modified from Bache *et al.*, 2015. Vertical exaggeration ×6.
Fig. 2. *(A) Croquis illustrant l'analyse de la subsidence du Bassin Provençal (modifié d'après Rabineau, 2001 and Leroux, 2012). (B) Profil sismique (en profondeur, km) (TGS-Nopec) traversant perpendiculairement le Bassin Provençal (localisation dans la Fig. 1) montrant les valeurs de la pente de la base du sel (en pointillés violets) sur la pente inférieure et dans le bassin profond.*

topography (Fig. 2). The Messinian units in the Provençal Basin mainly occupy the lower slope and the deep basin (Figs. 2, 3): the present-day salt deposit accumulated in the deep basin and lower slope, where it onlapped the pre-salt sequences (Fig. 2). The salt transparent acoustic facies is interpreted as predominantly consisting of halite (Lofi *et al.*, 2011). The UU is the most recent Messinian unit and is composed of a set of parallel and relatively continuous reflectors of high amplitude overlying the salt (Lofi *et al.*, 2011) (Fig. 5). In the upper slope and shelf, we observed the Messinian Erosional Surface (MES, Lofi *et al.*, 2011), which is considered the top of our pre-salt unit or the base of the Pliocene-Pleistocene sequence (Fig. 3).

3 Salt tectonics and crustal setting history

3.1 Crustal segmentation

Figure 4 shows the evolution of the basin and its margins using three key ages (∼16 Ma, ∼5.6 Ma and 0 Ma). The deep crustal segmentation, geometry and nature are taken from the wide-angle refraction profiles (so in depth) interpreted in Moulin *et al.*, 2015 and Afilhado *et al.*, 2015. The profiles show the crustal geometry, segmentation, and nature with respect to

salt deposition during the MSC and the present-day salt morphologies.

Around 16 Ma (Fig. 4a) the rotation of the Corso-Sardinian block has ceased, and the Provençal Basin assumed the shape and boundaries that are still visible today (*e.g.* Auzende *et al.*, 1973; Olivet, 1996; Bache *et al.*, 2010): no major horizontal movements have occurred from this time to the present-day. Since the formation of oceanic crust, subsidence in the deep basin (within the oceanic and transitional domains) is purely vertical while in the thinned continental crust domain, the authors observed a tilting seaward (Rabineau *et al.*, 2014; Leroux *et al.*, 2015a, 2020b) (Fig. 4a). Pre-Messinian sedimentation is characterised by marine deposits filling the basement roughness (Fig. 2).

Around 5.6 Ma (Fig. 4b) (Clauzon *et al.*, 1996; CIESM, 2008; Gorini *et al.*, 2015), a major sea-level drop (>1000 m) took place leading to the salt deposition: it thus occurred in a closed and already formed basin context, after the opening of the basin, above a thick pre-Messinian sedimentary blanket. The salt deposited in the deep basin, pinching out on the pre-salt sediments in the lower slope. The initial thickness of salt can be considered constant in the deep basin while it may decrease at the basin edges. Today, salt morphologies in the deep basin show substantial differences (Bellucci *et al.*, 2021a), due to the evolution of salt tectonics over the last ∼5 million years (Fig. 4c).
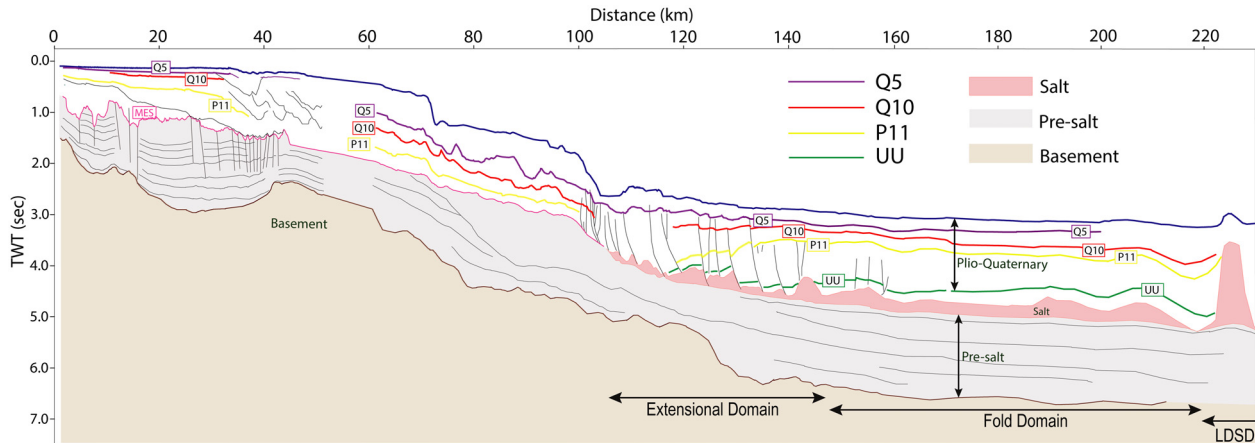
Fig. 3. Seismic line-drawing illustrating, from the shelf to the deep basin, the Messinian and Pliocene-Pleistocene markers used in this study. The pre-salt unit is considered as the mega-sequence below the salt (in the deep basin) or below the Messinian Erosional Surface (in the upper slope and shelf) (modified after Leroux *et al.*, 2019). Salt morphology domains from Bellucci *et al.*, 2021a. LDSD refers to Large Diapirs Salt Domain.
Fig. 3. *Ligne sismique illustrant, depuis le plateau continental jusqu'au bassin profond, les marqueurs messiniens et pliocènes-pléistocènes utilisés dans cette étude.*

3.2 Present-day salt morphologies in the Provençal basin

From the lower slope to the deep basin, the Provençal margin shows salt structures outlining three different kinematic domains, as also described by previous authors (Gaullier, 1993; Gorini, 1993; Dos Reis *et al.*, 2005; Mianaekere *et al.*, 2020a, 2020b).

– The Extensional domain is characterised by listric basinward-dipping faults that develop from the base of the salt in overlying units (Fig. 6). This domain is characterised by salt rollers and rollover structures (Fig. 6). The salt rollers describe low-amplitude deflections of the upper surface of a salt layer at the lower termination of normal faults in the overlying sediments (*e.g.* Jackson and Hudec, 2017). The growth faults are therefore syn-sedimentary. They may be still actively deforming the seafloor (Dos Reis *et al.*, 2005; Badhani *et al.*, 2020) or be buried (Fig. 7). Clear growth sequences in the Pliocene and Pleistocene deposits are represented in Figure 6. The Extensional domain is interpreted in the lower slope, occupying an area that extend from the upslope limit of salt up to 70 km basinward (Fig. 7), coincident with the deep hinge line separating two different crustal domains with two different modes of subsidence (Moulin *et al.*, 2015; Leroux *et al.*, 2015).

– The Fold domain is characterised by salt pillows, anticlines and tabular salt (Fig. 6) concordant with the overburden. The large-scale deformation associated to salt pillow affects the seafloor. Some outer-arc extension faults are locally observed over the roof of salt and mostly above the UU. An area of greater salt thickness (between latitude 41°−42°N and longitude 4°−5°E) of around 900-1100 m (with a salt velocity of 4.5 km/s) (Fig. 7) is indicated within this domain. The anticlinal axes highlight a NE-SW direction or, when involved in the Petit Rhône Fan, the axis directions follow the main sedimentary path (mainly N-S and NW-SE).

– The Large Diapir Salt Domain (LDSD) is characterised by salt walls and stocks (Fig. 6) clearly showing truncation and onlaps within the overburden. Its landward limit is coincident with the limit of two different crustal domains (exhumed lower continental crust versus proto-oceanic crust; Moulin *et al.*, 2015) (Bellucci *et al.*, 2021a). The salt walls show a preferential N-S direction as well as the mini-basins located between the salt structures (plot direction Fig. 7). The mini-basins (Fig. 6, Fig. 7) form preferential pathways for sediments, confirming the mutual relationship between sedimentation pathways and salt tectonics (Dos Reis, 2001). The salt structures are growing and deforming the seafloor (see inset in Fig. 6). The large salt walls and stocks become narrower and less piercing towards S-W (Fig. 6). Here, the diapirs occasionally deform the seafloor and are more connected, making it more difficult to individually identify them on salt thickness map.

4 Dataset and method

We used a large dataset of reflection seismic surveys (Fig. 1) including both academic and industrial seismic lines acquired since the 1960s, coupled with several boreholes in the platform and slope. The available reflection seismic dataset, a result of collaboration between French, Spanish, Algerian and Italian research institutes, covers most of the Western Mediterranean sub-basins except for the Ligurian Basin (see also the seismic stratigraphic compilation in Bellucci *et al.*, 2021b. All the seismic lines details can be found in Leroux, 2012 and Bellucci, 2021. In this work, we have concentrated in the Provençal Basin. The seismic interpretation were undertaken using the principles of seismic stratigraphy (Vail *et al.*, 1977) with recognition of seismic facies, seismic unit identification based on the configuration of seismic reflectors, including reflector continuity and termination (onlaps, downlaps, toplaps). We jointly interpreted different resolution lines in time domain, from very low (*e.g.* ECORS survey; Gorini
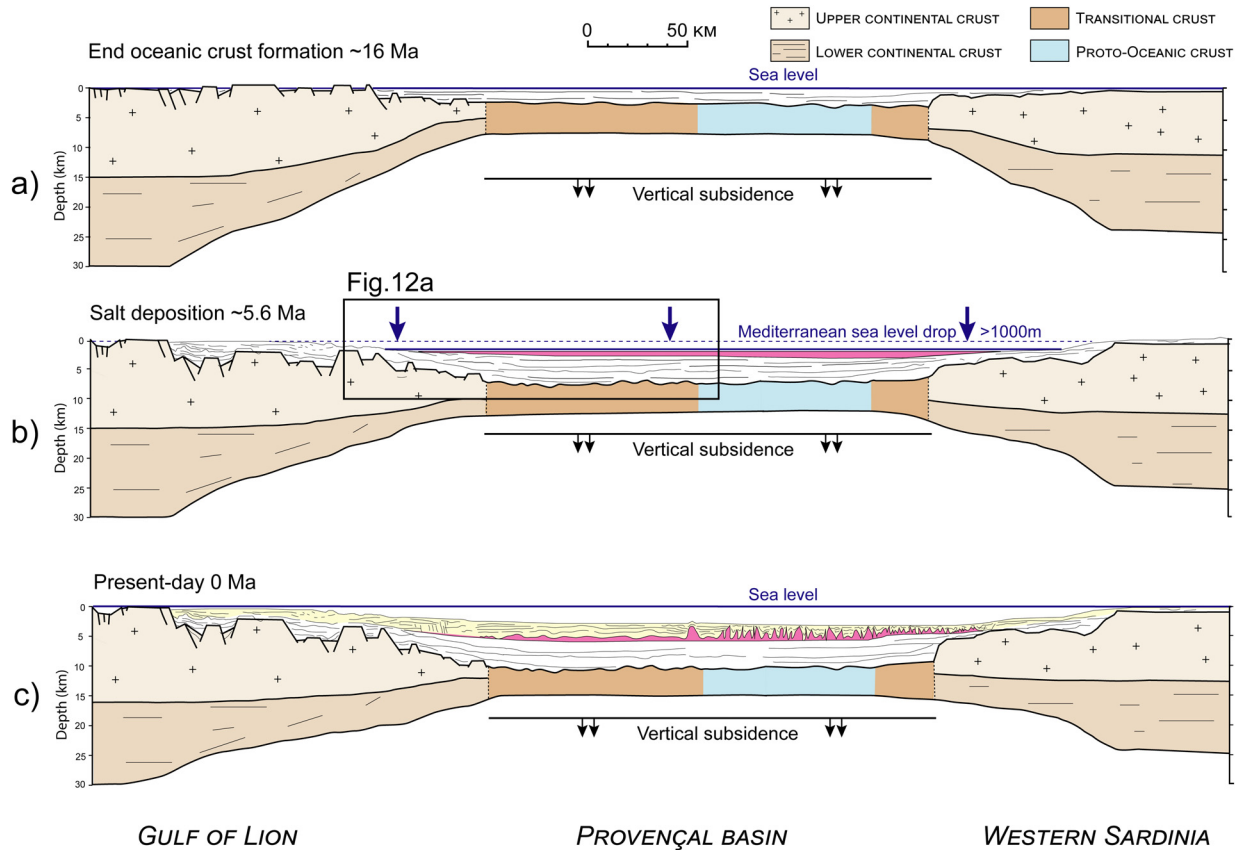
Fig. 4. Sketch illustrating the Messinian salt deposition compared to the subsidence evolution in the Gulf of Lion, Provençal Basin and Western Sardinian conjugated margins. (a) Basin reconstruction at 16 Ma: the Corso-Sardinian block ceased the counter-clockwise rotation; the deep basin, composed by proto-oceanic crust and bordered by transitional crust, (Moulin *et al.*, 2015; Afilhado *et al.*, 2015) is characterized by a vertical subsidence. (b) Basin reconstruction at ~5.6 Ma: the Messinian sea-level drop took place leading to the salt deposition above a thick pre-salt sequence. The initial salt thickness is considered constant except on the margin edges. (c) Basin reconstruction at present-day: after the reflooding and the end of the MSC (5.32 Ma) the Pliocene-Pleistocene sedimentation filled the basin and margins. Wide variations in salt morphologies are observed at present-day.

Fig. 4. Croquis illustrant le dépôt de sel messinien comparé à l'évolution de la subsidence dans le Golfe du Lion, le Bassin Provençal et la marge conjuguée de la Sardaigne occidentale. a) Reconstruction du bassin à 16 Ma. b) Reconstruction du bassin à ~5,6 Ma. c) Reconstruction du bassin à l'époque actuelle.

et al., 1993) to very high (*e.g.* PROGRESS survey; DOI: 10.17600/3020080). Isochron maps (TWTT) were then computed with the nearest neighbour interpolation algorithm, which assigns a weighted average value to each node that has one or more data points within a search radius (0.5 km). The radius was chosen based on the maximum average distance between lines in the dataset. Then isopach maps (in TWTT) were also calculated. The time-isopachs maps are used as a first order approximation as velocities in one unit would change according to present-day depth of the unit (with higher velocities when unit is deeper). Full time-depth conversion could not be done on all the dataset due to the limited available depth seismic data and limited information on true velocities in 3D (Leroux, 2012). However, simple time-depth conversion was applied locally (within one single unit) using average velocities (from the unit) (see Supplementary Data) to give a first approximation of thicknesses in meters. Seismic two-way travel-time (TWT) has generally been tied to formation tops in wells using velocities from sonic logs. Note that those

time-depth relationships are published in Bache *et al.*, 2015 (Fig. 2) and Leroux, 2012 (including velocities from refraction) (All the velocities information are provided in the two Supplementary Data figures).

4.1 Age of reflectors

In addition to the base and top salt reflectors, we have interpreted the Messinian margin Erosional Surface (MES) in the shelf and upper slope, and the top of the UU in the lower slope and deep basin, both generally dated at 5.33 Ma (CIESM, 2008) and indicating the end of the Salinity Crisis. Considering that an exact age and duration for salt deposition are still debated (*e.g.* Clauzon *et al.*, 1996; Bache *et al.*, 2012; Meilijson *et al.*, 2019), we assumed a salt deposition started around 5.6 Ma (Fig. 5). Some Pliocene-Pleistocene key reflectors previously interpreted on the shelf in the work of Rabineau 2001, Leroux 2012 and Leroux *et al.*, 2017 have
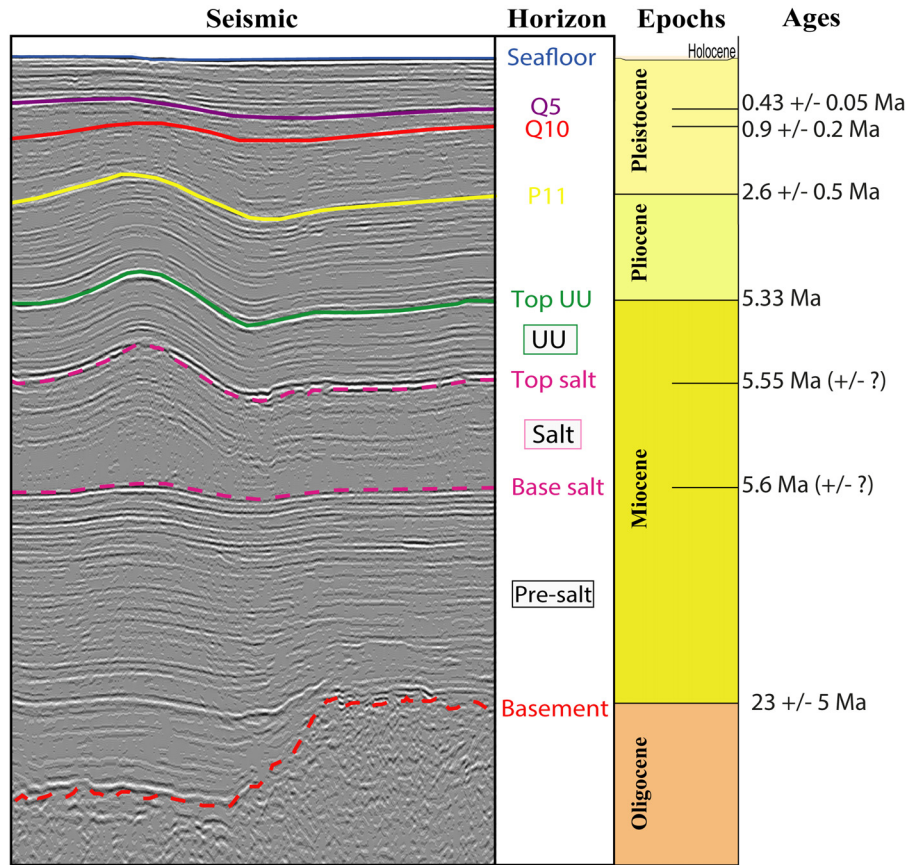
Fig. 5. Seismic reflectors and relative ages used in this study. From left to right, a seismic zoom in the deep basin with reflectors interpretation, name, epoch, and age. Pliocene-Pleistocene reflectors have been extended in the lower slope and deep basin from works of Leroux 2012 and Rabineau 2001. MSC terminology, limit and ages are from CIESM, 2008 and Lofi *et al.*, 2011.

Fig. 5. *Réflecteurs sismiques et âges relatifs utilisés dans cette étude. De gauche à droite, un zoom sismique dans le bassin profond avec interprétation des réflecteurs, nom, époque et âge.*

been extended in the deep basin. From the oldest to the youngest, the Pliocene-Pleistocene reflectors are labelled P11, Q10 and Q5 (Fig. 5). P11 is a strong erosional discontinuity dated from Autan1 borehole (location in Fig. 1B) at 2.6 ± 0.5 Ma (Fig. 5) thanks to the appearance of *Neogloboquadrina atlantica* (planktonic foraminifer), used to date the base of the Gelasian (2.588 Ma; *i.e.* the base of Pleistocene in marine environments, Suc *et al.*, 1992). The Q5 surface, dated at 434 ± 5 kyr (Rabineau *et al.*, 2006; Bassetti *et al.*, 2008; Sierro *et al.*, 2009; Leroux *et al.*, 2017) is part of the last five shelf erosional surfaces corresponding to the last five glacial maxima that correlates to a correlative conformity surface on the outer shelf and upper slope. The last most recent glacial maxima 20 ka) has been fully dated in its correlative conformity part using C^{14} dating (*e.g.* Rabineau *et al.*, 2005). Q5 was interpreted as the glacial maxima related to MIS 12 (Marine isotopic Stage 12 at 434 ± 5 kyr), initially by considering architecture of deposition and numerical simulation (Rabineau *et al.*, 2005 and 2006) (glacial Maxima). This dating is now fully proved by results from the two PROMESS drill-sites (Fig. 1B) (with nannofossils and oxygen isotopes analysis) (Bassetti *et al.*, 2008; Sierro *et al.*, 2009). Q10 is another high seismic amplitude erosional discontinuity on the

shelf whose age is estimated at 0.9 ± 0.2 Ma based on stratigraphic correlations and numerical modelling (Fig. 5) (Rabineau, 2001; Leroux *et al.*, 2014; Rabineau *et al.*, 2014). The uncertainty on the Q10 surface is greater as no direct dating information are available.

4.2 Uncertainties

The seismic dataset used in this study consists of 2D lines which, although forming a dense seismic grid with few blank zones, can lead to several out of the plane signals in the presence of complex geological structures. Correlation of interpretation within different resolution can be sometimes tricky and lead to errors. The seismic interpretation was performed on TWT lines, in an attempt to minimize errors in the correlation between the few lines available in depth domain and those in TWT. The time domain implies being more cautious in using sedimentary thicknesses between units as an argument for dating deformation of the overburden over time (*e.g.* exaggerated thicknesses on the flanks of sloping structures). We mainly used stratigraphic terminations (onlap, toplap..) to determine the intensity and timing of the salt deformation and the accommodation of the overburden. The
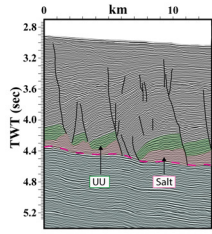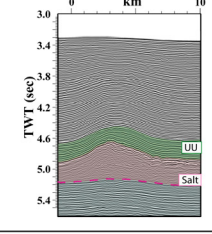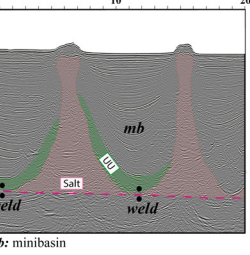
Name	Description	Seismic example	Min Lenght	Min Height	Related structures
Extensional domain	Extensional domain located at lower continental slope, characterized by thin-skinned tectonics. The listric domain is characterized by salt rollers, rollover anticlines. They generated from regional extension due to basinward salt flow. Basinward dip of the base of salt. Listric faults, locally still active. Trasparent to chaotic salt seismic facies.		1 km	200 m	Basinward dip of the listric faults into Upper Unit and Plio-Quaternary units. Faults do not displace the base of salt which it acts as a detachment surface. Clear growth sequences in the Pliocene deposits.
Fold domain	Wide base of salt (up to 5 km), absence of persistent diapirism. Pillow large scale deformation, locally affecting the seafloor. Overburden (including the Upper Unit) concordant with salt top. Absence of listric landward-dipping faults. Trasparent salt seismic facies.		5 km	300 m	Locally, outer-arc extension faults over the roof of salt, mostly located above the Upper Unit. Base of salt sub-horizontal and not faulted.
Large Diapirs salt domain	Salt wide base and piercing diapirism, active up to nowdays, forming salt stocks and walls. Discordant overburden. The salt structures deform the seafloor, form evolved minibasin and weld in the diapirs flanks. Transparent salt seismic facies. Upper Unit «compressed» or eroded at the top.		3 km	600 m	Locally, outer-arc extension faults over the roof of salt. Base of salt sub-horizontal and not faulted. Salt lateral expulsion induced minibasins subsidence and locally salt welds.

Fig. 6. Geometry description and related structures of present-day salt morphologies interpreted in the area of study. mb: minibasin.
Fig. 6. Description de la géométrie et de ses structures associées des morphologies actuelles du sel interprétées dans la zone d'étude.

Pliocene-Pleistocene reflectors often correspond to erosional surfaces and discontinuities on the shelf but were correlated as correlative conformities on the slope and deep basin. This correlation in the deep basin is also subject to some uncertainties as it is not always easy to conduct (especially when crossing faulted areas and piercing salt structures). The wells used for the verification of the seismic interpretations are mostly located on the shelf and upper slope (Fig. 1). The well-to-seismic tie therefore has an uncertainty that increases towards the deep basin, where the distance to the wells is greater and the salt deformation more discordant with the overburden. All this can lead to a locally varying uncertainty of the mapped isochrons, thickness and interpretation that we estimate in the range of a few tens of meters. Despite these uncertainties, the use of detailed markers provides an unprecedented seismo-stratigraphic background to discuss salt tectonics through time.

5 Results

5.1 Salt structures timing evolution

In this section we describe the evolution in time and space of salt tectonic structures in the Provençal Basin. We first describe the timing phases depicted on 2D profiles perpendicular to the margin and then extend our observations in space with detailed isochrons maps of the Pliocene-Pleistocene sequences. The timing phases described below were discriminated solely based on the geometry observations and not by considering the causes and drivers that led to their formation. Main parameters used are the stratigraphic terminations, the accommodation of the overburden (concordant or discordant on the salt structure) and the spatial change of the deformation style.

5.1.1 Phase 1 (Messinian): Early salt deformation in the deep basin

We have primarily focused on understanding the initial phase of salt deformation. The profile in Figure 8 (location Fig. 6) shows the evolution of salt structures from the fold to the large diapir salt domain. The UU sequence (green, Fig. 8) shows several parallel onlaps on salt within it (Fig. 8): zoom A' displays several reflectors within the UU with clear onlaps and an unconformity that is locally faulted and regionally parallel to the Pliocene-Pleistocene layers. In the lower part of the UU, the reflectors are not parallel to each other nor to the overlying layers of the Pliocene. The onlaps terminations seem to be mainly located in the lower-middle part of the UU sequence: the two to three reflectors above the salt follow the salt top deformation while just above them the growth episodes appear. As the top salt can be locally difficult to define, we do not exclude that the deepest UU reflectors are onlapping the salt.
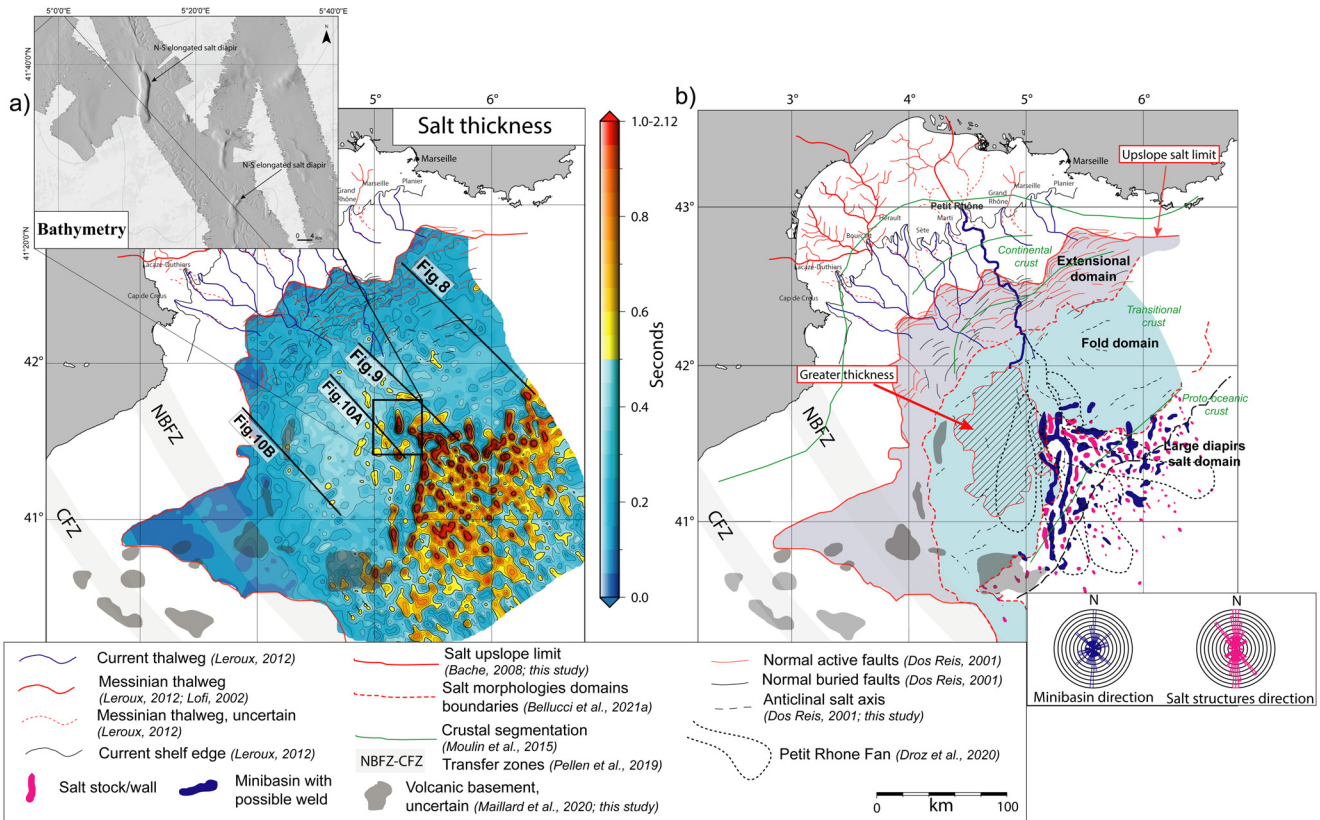
Fig. 7. (a) The salt vertical thickness (isopachs) map shows regional discontinuity variation in the basin, corresponding to salt-structures distribution. (b) The identified salt morphology domains are interpreted as well as other structural elements. The present-day and Messinian thalwegs are from Leroux 2012 and Lofi 2002. Transfer zones are from Pellen *et al.*, 2019. Grey polygons represent uncertain volcanic basement from Maillard *et al.*, 2020 and this study. Faults are from Dos Reis 2001). Red polygon filled with black lines represents the greater salt thickness area in the fold domain. Green lines represent the crustal segmentation (from Moulin *et al.*, 2015. The plots in the bottom-right corner display the main minibasins and salt walls direction in the LDSD. Petit Rhône Fan is from Droz *et al.*, 2020. Top left inset shows a detail of the bathymetric expression of two N-S oriented diapirs. NBFZ: North Balearic Fault Zone. CFZ: Catalan Fault Zone.
Fig. 7. *(a) La carte d'épaisseur verticale du sel (isopaches) montre une discontinuité régionale dans le bassin, correspondant à la distribution des structures salifères. (b) Les domaines de morphologie du sel identifiés sont interprétés ainsi que d'autres éléments structuraux.*

These observations suggest an early salt deformation in the deep basin, starting during the last phase of the MSC deposition (UU sequence) or last phase of MU deposition.

Phase 1 (early salt deformation) is only well imaged on the fold domain (Fig. 8). Basinward, in the LDSD, the early salt deformation is difficult to discriminate. Here, the vertical stocks and walls inhibit small-scale deformation, and the UU could be interpreted as a pre-kinematic layer (*e.g.* Mianaekere & Adam, 2020a). Nevertheless, given the observed onlaps within the UU in 2D transects (Figs. 8, 9, 10 A-B) we suggest that salt began to deform during UU deposition throughout the deep basin, also within this domain. Phase 1 was thus active during UU deposition, and may have been started earlier, during salt deposition (~5.6-5.33 Ma).

5.1.2 Phase 2 (Pliocene)

The Extensional domain is characterized by basinward-dipping listric faults (Figs. 6, 8) typical of thin-skinned salt tectonics, *i.e.* affecting only the salt and the overlying

deposits (*e.g.* Cobbold and Szatmari, 1991). To reconstruct fault-evolution timing, it is necessary to recognize the growth strata, induced in this case by fault activity. The parallel UU reflectors involved in the salt rollers (black arrows, zoom B', Fig. 9) and the almost total absence of onlaps suggest an activation of the listric faults after its deposition, thus after or from the Lower Pliocene onwards. The UU sequence was already fully deposited at the time of fault initiation, whose age therefore spans from the Lower Pliocene to the present-day, as confirmed by seafloor deformations (also according to Badhani *et al.*, 2020; Droz *et al.*, 2020) and several post-Messinian growth strata (red arrows, fig. 9-zoom B'). The beginning of listric fault activity in the lower slope (Early Pliocene) is therefore subsequent to the salt deformation of phase 1 in the deep basin, which occurred in the Late Messinian. Phase 2 began in the Early Pliocene and ended around the Pliocene-Pleistocene boundary (5.33 − ~2.6 Ma) (Figs. 8, 9, 10 A-B).

In the N-E sector of the fold domain (Figs. 8, 9, 10 A-B), the growth of pillows continued during all the Phase 2. In the yellow unit, the number of reflectors decreasing in the anticline
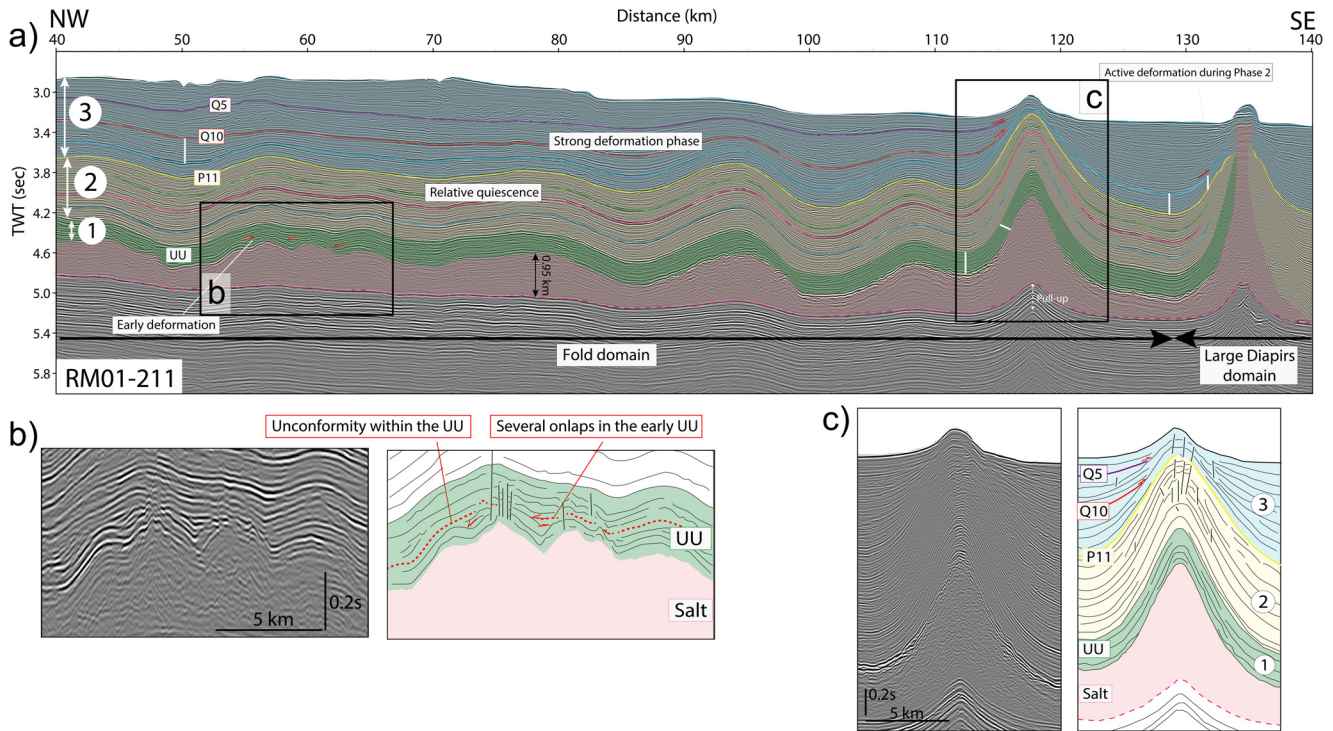
Fig. 8. (a) Seismic profile crossing the N-E sector of the Gulf of Lion. The three stratigraphic intervals depicted in this work are shown. (b) Zoom showing the suggested early salt deformation in the lower part of the UU, testified by several onlaps within it. (c) Basinward zoom shows the deformation of UU and Pliocene-Pleistocene units when involved in anticlinal-like deformation. Encircled numbers indicate the salt tectonics phases: refer to text for more details.

Fig. 8. *(a) Profil sismique traversant le secteur nord-est du Golfe du Lion. (b) Zoom montrant la déformation précoce du sel dans la partie inférieure de l'UU. (c) Le zoom vers le bassin montre la déformation de l'UU et des unités pliocènes-pléistocènes lorsqu'elles sont impliquées dans une déformation de type anticlinal.*

limbs compared to the synclinal part (from about 15 to 9) and some onlaps within it attest a growth rate that seems to be more intense in the deep basin (basinward part of the fold domain) (Fig. 9–zoom B"; Fig. 8–zoom A").

In the LDSD, phase 2 reflectors onlap the salt diapirs, gently folding following the upward deformation (Figs. 8, 9, 10 A-B). The overlying sequences are discordant and syndiapirism. The LDSD structures probably underwent a passive evolution during phase 2. The structures grew towards the surface (currently lacking or having a thin overlying sedimentary sequence) at the same time as the mini-basins on the diapir side were sinking.

5.1.3 Phase 3 (Pleistocene – Present-day)

Phase 3 is the most significant deformation phase in the Provençal Basin (Figs. 8, 9, 10 A-B). It started at the end of the Pliocene, Early Pleistocene (~2.6 Ma) and is still active.

The Extensional domain is characterised by basinward-dipped listric faults, salt rollers and rollover structures. The salt glides along its detachment surface, concomitant with the growing of the listric faults. Regionally, the still active faults are located in the basinward part of the Extensional domain, while those buried (inactive) are localised in its landward sector (Fig. 6), as also mentioned by Dos Reis 2001. This observation suggests that the salt gliding and subsequent fault activity started in the Early Pliocene (phase 2) but are still

active today. The progressive basinward gliding of the salt led to the welding of the primary salt layer and cessation of fault movement upslope the Extensional domain. Instead, downslope of this domain, the faults are still active testifying to a gravitational gliding of the salt until the present-day. As previously mentioned, the deformation is mostly thin-skinned. However, an important base of salt displacement is observed in figure 10B, where the salt is thickened in correspondence of a volcanic structure (Maillard *et al.*, 2020). The compressional salt thickening in the updip side caused an increase in gliding velocity in the downdip sector, resulting in the formation of listric faults and growth strata (see also Dooley *et al.*, 2017). In the updip part, the Pliocene and Pleistocene units show syn-deformation deposition, which may be caused by progressive thickening of salt (given by the continuous gliding from the mid-slope) with consequent deformation above the volcano. An almost constant UU thickness indicates predominantly active gliding from the Lower Pliocene onwards.

The salt-cored folds continued growing throughout phase 3 within the entire domain, as attested by several onlaps (Figs. 8, 9, 10 A-B) observed within it. In the central sector of the Fold domain, the pillows are more deformed, especially at the limit with the LDSD (Figs. 8, 9, 10 A-B).

In the LDSD domain, as in phase 2 (yellow colour sequence), phase 3 reflectors (blue sequence) are discordant
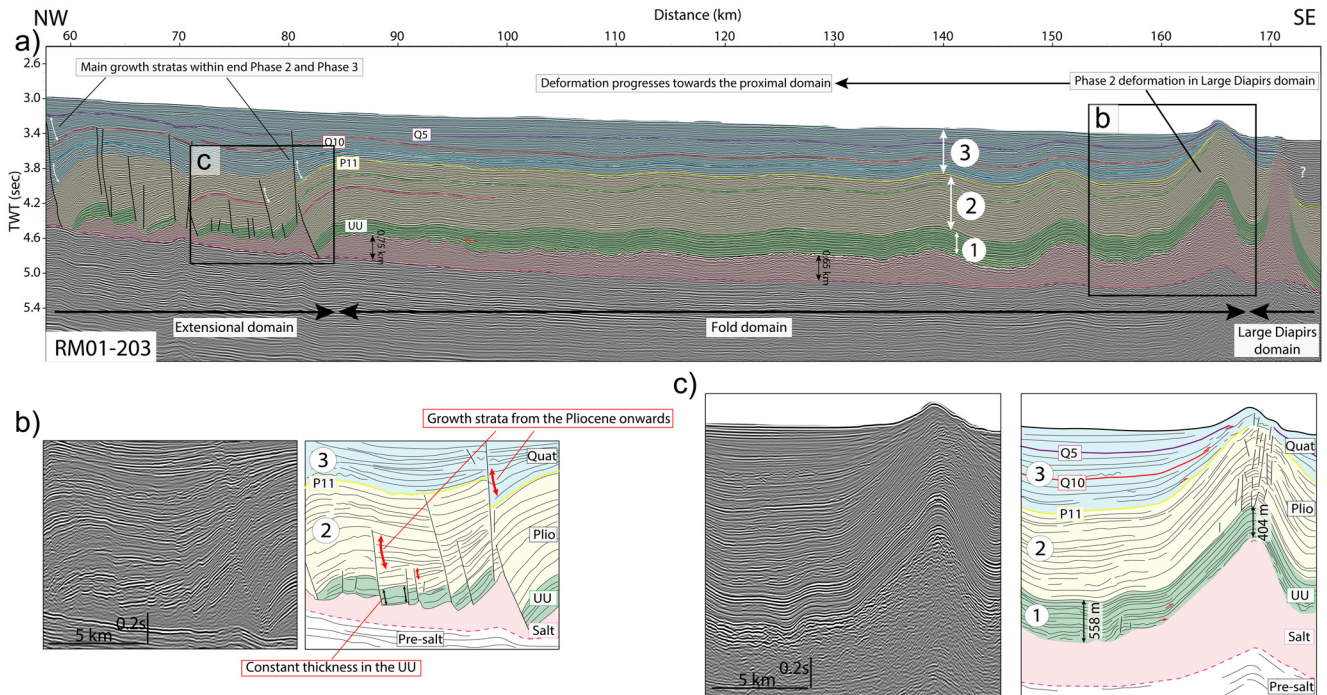
Fig. 9. (a) Seismic profile crossing the N-E sector of the Provençal Basin. The three stratigraphic intervals depicted in this work are shown. (b) Zoom showing the active growth strata starting from the Lower Pliocene onwards, after the complete deposition of the UU.) Zoom showing the boundary between the fold and the large diapir salt domains. Note the thickness variation within the UU (green), the almost constant thickness during phase 2 (yellow sequence) and the clearly thickness variations during phase 3 (blue sequence). An average velocity of 3,850 m/s (Leroux, 2012; Supplementary Data 1-2) is used to calculate a first order estimation of UU thickness. Encircled numbers indicate the salt tectonics phases: refer to text for more details.

Fig. 9. (a) *Profil sismique traversant le secteur nord-est du Bassin Provençal. (b) Zoom montrant les growth strata à partir du Pliocène inférieur, après le dépôt complet de l'UU. (c) Zoom montrant la frontière entre le Fold domain et celui de LDSD.*

with the salt diapirs, onlapping them. The salt deformation rate increases at this phase, especially in the fold domain.

5.2 Evolution of the salt deformation in the margin

Figure 11A represents the sedimentary isopach map (TWTT) of the Pliocene unit whose age ranges from the end of the MSC (5.33 Ma) to the P11 reflector (~2.6 Ma) (corresponding to phase 2). During the Early Pliocene, the sedimentary inputs filled the subaerial canyons formed during Messinian erosion (up to 1000 m deep; Clauzon, 1982), both on land and up to the present-day outer shelf location, which also emerged at that time (Leroux, 2012). Once the sediments had filled the Messinian canyons, they spread into the deep basin via a slope bypass (Fig. 11A). The sedimentary thickness is greatest in the north-eastern sector of the fold domain (Figs. 8, 9, 11A), while it decreases towards the S-W (Figs. 10 A-B, 11 A). The mapped sedimentary unit (MSC-P11; 5.33-2.6 Ma) corresponds to phase 2 of the salt deformation described in this work. The salt tectonics phase 2 is characterised by basinward-dipping listric fault formation in the Extensional domain, more quiescent deformation phase in the present-day fold domain and active, intense deformation within the LDSD. The constant thickness in the N-E sector of the fold domain (Fig. 11A) confirms a period of relative salt tectonic quiescence in this area while, as observed in profile 10B, in the S-W sector, deformation is stronger since the Lower Pliocene. In the LDSD sedimentary depocenters within the

mini-basins suggest active deformation throughout phase 2 (Fig. 11A). In the fold domain, because the significant input of Pliocene sedimentation, the salt does not appear to have deformed as intensely and rapidly as it has in the LDSD. The large sedimentary input at this stage may have slowed the deformation. In the S-W sector, characterised by a much lower sedimentary thickness (Fig. 11A), the salt deformed prematurely.

During the Pleistocene (Phase 3), strong turbidite sedimentation occurred and led to aggradation and progradation of thick turbidite systems linked to the main canyons on the Gulf of Lion (*e.g.* Dos Reis, 2001; Droz *et al.*, 2020; Badhani *et al.*, 2020). The main source is the Rhône, which mainly feeds the canyons of Sète, Marti, Petit-Rhône and Grand Rhône. The doubling of sedimentary volume at 0.9 Ma, coinciding with the Mid-Pleistocene Climatic Revolution, is characterised by a large amount of continental terrigenous input, a change in cyclicity and higher sea-level amplitude variations that facilitate connections between onshore rivers and offshore canyons (Leroux, 2012) (Fig. 11B). The isochron map in Figure 11B illustrates the resulting sediment deposits on the youngest part (0.9 Ma-0) of phase 3 of salt deformation (estimated in this work between 2.6 and the present-day) and aims to illustrate in detail the sedimentary arrival caused by the Rhône at 0.9 Ma. Phase 3 is characterised by intense salt deformation both in the fold domain, with the acceleration of salt rising in pillow structures, and in the LDSD, where diapirs deformed vertically with a passive character (see Rowan and Giles, 2021; Jackson and Hudec, 2017). In the LDSD, the
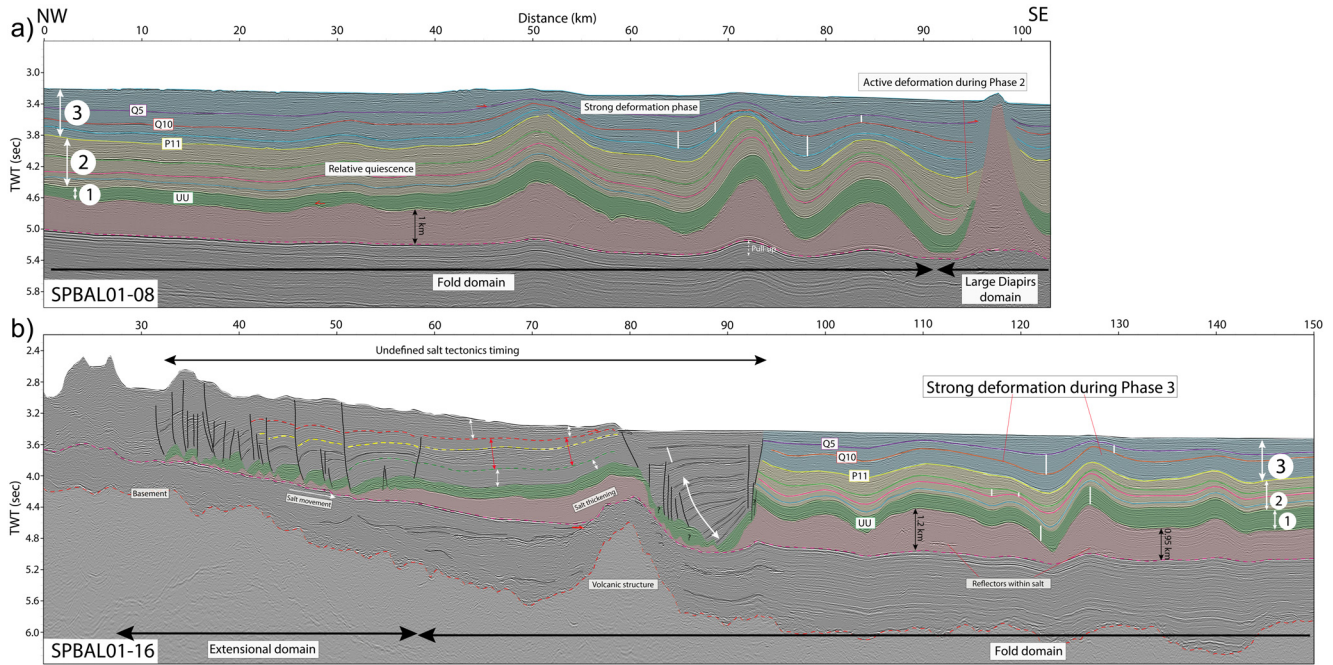
Fig. 10. (a) Seismic profile crossing perpendicularly the central sector of the Provençal Basin. The three stratigraphic intervals depicted in this work are shown. Note the greater salt thickness compared to profile in figures 8, 9. (b) Seismic profile crossing the S-W sector of the Provençal Basin. Encircled numbers indicate the salt tectonics phases: refer to text for more details.

Fig. 10. *(a) Profil sismique traversant perpendiculairement le secteur central du Bassin Provençal. (b) Profil sismique traversant le secteur sud-ouest du Bassin Provençal.*

diapirs were subject to passive diapirism from the earliest stages of deformation, except for the Early Pliocene phase 2 in which the salt probably broke through the overburden. After that, the diapirs grew near-surface, syn-depositional, with a thin roof top. The Extensional domain is characterised by the evolution of the basinward-dipped listric faults, already active during phase 2. Pillow sizes do not appear to show significant differences between the different sectors (S-W and N-E, fig. 6). Salt thickness increases towards the S-W (Fig. 6a), as shown in the perpendicular profiles (salt thickness in figs. 8, 9, 10 A-B). The present-day directions of the salt structures and associated mini-basins in the LDSD show the same direction as the Petit-Rhône fan, aligned in an N-S and NW-SE (Figs. 8; 11B).

6 Discussion

In the Provençal Basin, the geometrical correlation between the Ocean-Continent transition and the variation in salt structures was already observed by Pautot *et al.,* 1984 and Le Cann 1987. Bellucci *et al.,* 2021a have recently confirmed that salt structures changing morphologies at the boundary between different crustal natures can be observed both in the Western Mediterranean but also in other salt-bearing passive margins. One of the objectives of this work is to further investigate this observation, detailing the relationship between the evolution of salt structural styles in time and space and the nature of underlying crust.

Three main salt tectonic phases were dated using previous stratigraphic markers (P11, Q10, Q5) whose dating and suitability were constrained by well data and numerical modelling. These phases are then geometrically related to the

underlying crustal nature, showing different salt structure features and the growth deformation rate with respect to their position above the crustal segments.

Figure 12 summarizes the salt structure deformation in the study area within the deep regional crustal evolution previously highlighted (Fig. 4). It shows the salt deformation evolution from the lower slope to the deep basin. We considered an almost constant initial salt thickness deposited above a flat Miocene surface. Salt pinches out on pre-salt Miocene sediments, mainly formed by detrital deposits resulting from erosion due to rapid desiccation (Clauzon *et al.*, 1996; Lofi *et al.*, 2005, 2011,). On the lower slope, salt is considered less thick than in the deep basin, pinching out on the edge of the basin. The thick (up to 2.5 km, fig. 2), unfaulted pre-salt sequence and the thin-skinned salt tectonics recorded over the entire margin seem to rule out, for its entire history, a regional tectonic influence on salt deformation, unless locally (Fig. 10B).

The hinge line highlighted in Figure 12 is located between the domain of tilting subsidence on the slope and the purely vertical subsidence in the deep basin (Rabineau *et al.*, 2014; Leroux *et al.,* 2015a). This hinge line also corresponds to the basinward boundary of the crustal necking domain, at the edge of the transitional domain (Fig. 12) (Moulin *et al.*, 2015; Leroux *et al.*, 2015a).

Subsequent to deposition (phase 0), the salt tectonic phase 1 is concomitant with UU deposition (~5.6–5.33 Ma) (or probably started during late MU deposition) and the initiation of deformation in the form of large pillows in the deep basin, away from the margin, above the proto-oceanic domain and the seaward sector of the transitional crust domain
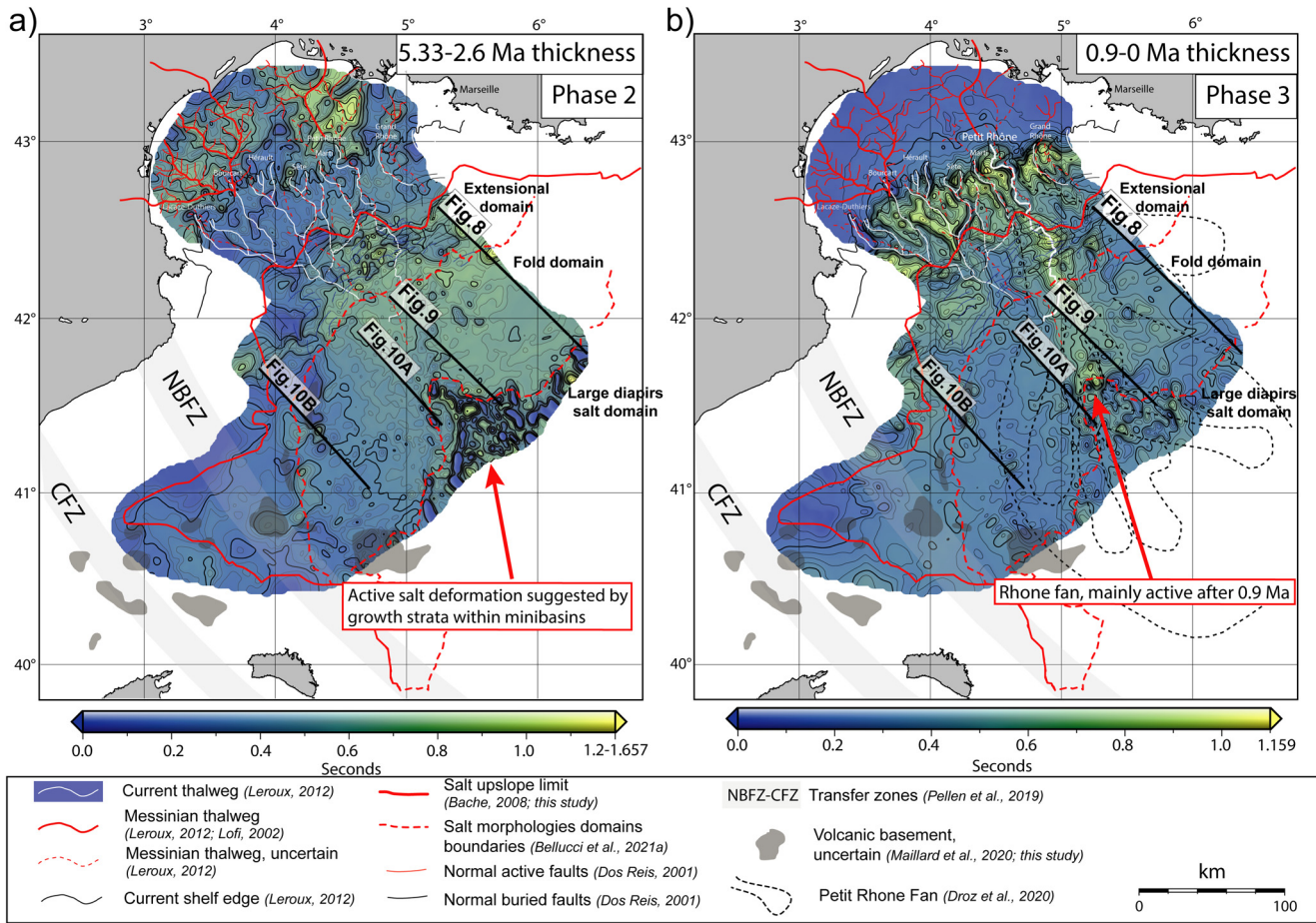
Fig. 11. Isochrone maps (in TWTT seconds) of the main Pliocene-Pleistocene units in the Provençal Basin. (a) The MSC-P11 TWTT-thickness (5.33-2.6 Ma) map corresponds to the salt tectonics phase 2, characterized by the formation of the listric faults in the extensional domain. (b) Q10-SB (0.9-0 Ma) TWTT-thickness map corresponds to the youngest part of the salt tectonics phase 3 described in this work, characterized by an intense deformation and orientation of the salt structures in the present-day Rhône thalweg direction. The profiles are shown in Figures 8, 9 and 10.

Fig. 11. Cartes isochrones (en secondes TWTT) des principales unités pliocènes-pléistocènes dans le Bassin Provençal. a) La carte d'épaisseur TWTT du MSC-P11 (5,33-2,6 Ma) correspond à la phase 2 de la tectonique salifère. b) La carte d'épaisseur TWTT du Q10-SB (0,9-0 Ma) correspond à la partie la plus récente de la phase 3 de la tectonique salifère décrite dans ce travail.

(Fig. 12b). The first salt tectonic phase is the most difficult to investigate because it is the oldest and mildest of the three observed. Early deformation (since the first phase of salt deposition) has been discussed in the Western Mediterranean by several authors (*e.g.* Gaullier *et al.*, 2014; Soto *et al.*, 2022; Blondel *et al.*, 2022). Since the deformation started in the flat, horizontal deep basin and the listric faults are only active later (since the Lower Pliocene), we exclude that the gravitational gliding is the main trigger cause of the onset of salt deformation. We do not observe any thrusting of the salt base or underlying/overlying units that would suggest regional shortening that may cause early salt deformation, as for example described and quantified by Soto *et al.*, 2022;) in the Algerian Basin. The Provençal Basin, unlike the Algerian Basin, did not undergo regional shortening during the Messinian until the present-day. If we consider an initial constant salt and UU thicknesses, differential sedimentary loading also seems unlikely. Nevertheless, an almost imperceptible difference in UU thickness could trigger the formation of passive diapirism as long as the sedimentation

rate is not great enough to inhibit the process (see for instance Rowan and Giles, 2021 and Blondel *et al.*, 2022). The first phase of deformation is clearly observed only in the transitional crust domain. However, above oceanic crust, the UU pinching out onto diapiric structures suggests a syn-depositional subsidence and diapiric rise also in this domain. Here, early onlaps are currently hidden by a more intense evolutionary history.

Phase 2 (5.33–2.6/1.8 Ma) is characterised by the formation of listric faults in the lower slope (Fig. 12c). In the lower slope (present-day Extensional domain), the tilting subsidence has increased the base salt slope towards the deep basin, aiding both gliding of salt (leaving small remnant salt pillows on the slope), subsequent extension and formation of basinward-listric faults that dislocate UU sequences forming growth strata since the Lower Pliocene. During the same deformation phase, little deformation occurred above the fold domain (above the Transitional crust) while in the LDSD (above the proto-oceanic crust) the salt deformed more rapidly, passively and probably driven by updip extension. The
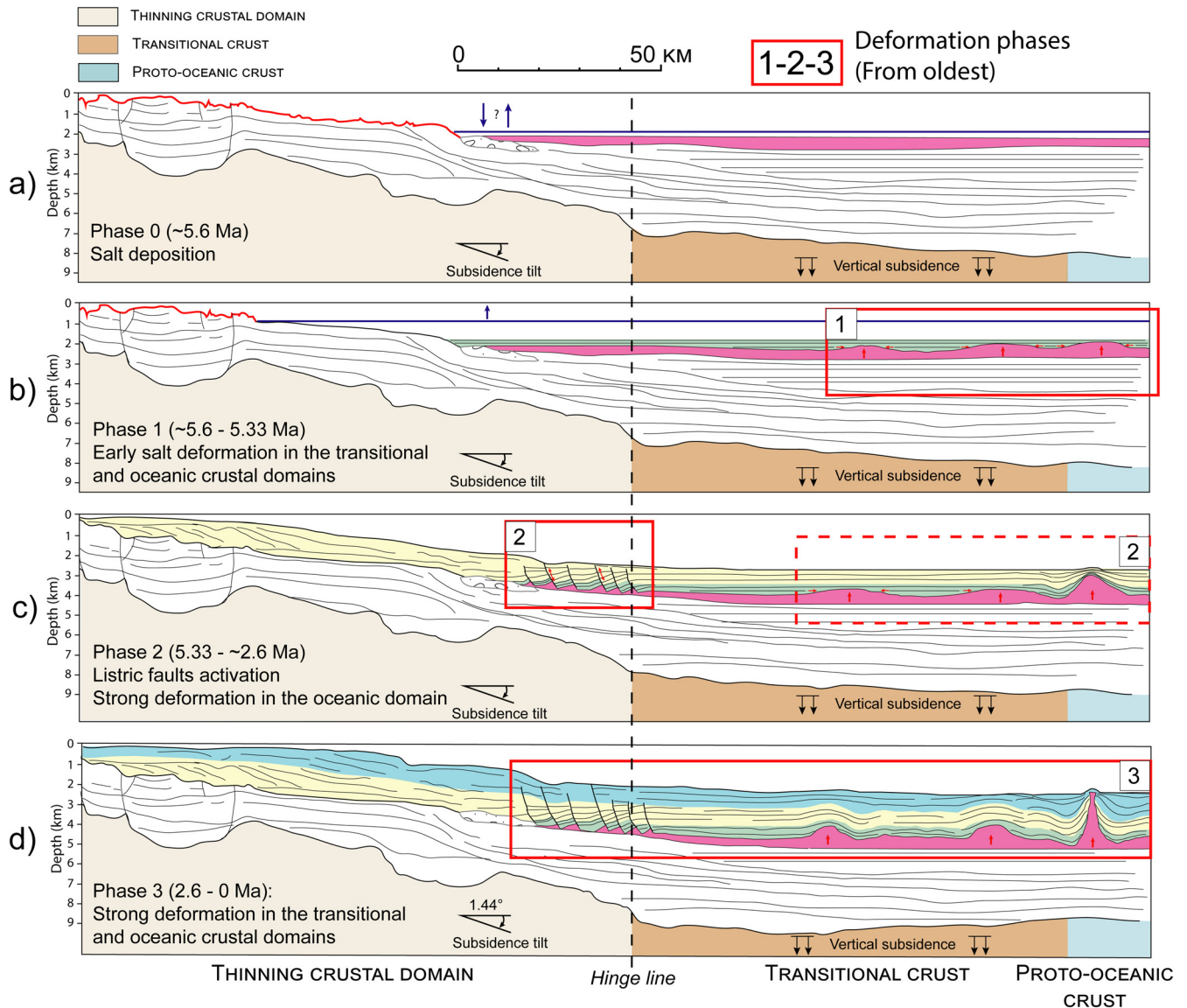
Fig. 12. Sketch illustrating the salt tectonics phases in the Provençal Basin. Red squares show the main deformation area for each phase. The Hinge line is taken from Leroux *et al.*, 2015a and marks the limit between a tilting subsidence on the slope and a purely vertical subsidence in the deep basin Rabineau *et al.*, 2014, Leroux *et al.*, 2015a. (a) Phase 0: Salt deposited in the deep basin and lower slope. The thickness is overall constant except in the margin edges. (b) Phase 1: early salt deformation above the transitional and oceanic crust domains during the UU deposition. (c) Phase 2: movement onset of the listric faults in the lower slope, relative quiescence above the transitional crust and start of passive diapirism above the oceanic crust. (d) Phase 3: greater salt deformation phase showing an active diapirism above the transitional crust and passive diapirism on the oceanic crust domain.

Fig. 12. *Croquis illustrant les phases de la tectonique salifère dans le Bassin Provençal. a) Phase 0 : sel déposé dans le bassin profond et sur la pente inférieure. L'épaisseur est globalement constante, excepté sur les bords de la marge. b) Phase 1 : Déformation précoce du sel au-dessus des domaines de croûte transitionnelle et océanique pendant le dépôt de l'UU. c) Phase 2 : Début du mouvement des failles listriques sur la pente inférieure, faible déformation au-dessus de la croûte transitionnelle et début du diapirisme passif au-dessus de la croûte océanique. d) Phase 3 : Phase de déformation plus importante montrant un diapirisme actif au-dessus de la croûte transitionnelle et un diapirisme passif sur le domaine de la croûte océanique.*

formation of listric faults in the lower slope during the Phase 2 is therefore subsequent to the formation of the first diapirs in the deep basin observed in Phase 1.

According to several authors, a few inclination degrees of the base salt (and top salt) would be sufficient to establish a gravity gliding regime (*e.g.* Duval *et al.*, 1992; Ings *et al.*, 2004; Brun and Fort, 2011). A depth profile perpendicularly

crossing the Provençal Basin (Fig. 2) highlights a slope base of salt of around 0.1° basinward of hinge line 3. Landward, it currently shows a slope of 0.75° in the distal lower slope and 1° if we consider the whole Extensional domain. Although the angle of the base salt is not an absolute criterion to generate deformation − other characteristics may come into play (presence of fluids, overlying sedimentary thickness, initial

Table 1. Table representing the main reflectors for the respective Pliocene-Pleistocene and Messinian sequences. The colour, name, supposed/known ages, main features and salt tectonic phase description for each reflector are shown.

	Discontinuity	Seismic unit	Supposed/known age	Main features	Salt tectonics phase
	Seabottom (SB)		0 Ma	Terrigeneous sedimentation from main rivers through turbidite system linked to the main canyons or convergent system of canyons. The Quaternary is characterized by mass-transport deposits. Channel/levee complexes. Decrease in the detrital volume around 2.6 Ma and increase at 0.9 Ma.	*Phase 3:* Greater deformation phase in the Gulf of Lion and Provençal basin. Greater dislocation of the listric faults between P11 and Q5. Active diapirism on the Transitional crust domain and passive above the oceanic crust domain.
Pleistocene		SB-Q5			
	Q5		450 kyr		
		Q10-Q5			
	Q10		0.9 Ma		
		PXX-Q10			
	PXX		1.7 +/- 0.2 Ma		*Transition between phase 2 and phase 3:* relative quiescence on the Transitional crust and strong deformation in the oceanic crust domain.
		P11-PXX			
Pliocene	P11		2.6 +/- 0.5 Ma	Peak of detritic sedimentation during the Pliocene.	*Phase 2:* Relative quiescence in the Transitional crust domain in the NE sector, while pillow formation in the SW area. Start of passive diapirism above the oceanic crust domain. Beginning of listric fault movement on the slope.
	Prg5; Prg4; Prg3	TopUU-P11			
Miocene	Top UU		5.33 Ma	Terrigeneous peak concomitant with the Messinian Salinity Crisis due to the fluvial erosion related to the fall of the base-level of the Mediterranean Sea.	*Phase 1:* Early deformation above Transitional and Oceanic crust domains. Listric faults on the slope not yet active.
		Upper Unit			
	Top Salt		~5.55 Ma		
		Salt			
	Base Salt		~5.6 Ma		

salt thickness, lithology…) − active salt gliding seems to be possible in the Extensional domain only. The base salt slope angle in this salt domain has increased throughout its history due to the progressive tilting of the margin and the value recorded at the present-day is therefore the highest slope it has ever reached. On the contrary, in the deep basin, its slope has not changed, as the subsidence is still purely vertical today. Phase 2 is characterized by active diapirism in the transitional crust domain showing pillow-like structures similar to those observed today. Here, the large sedimentary input could be the cause of the slowdown in the evolution of salt structures. The morphologies transition is sharp in oceanic crust, where salt diapirism mechanism is passive as early as Phase 2. Above the oceanic crust, salt broke early (probably as soon as Early Pliocene) through its UU roof and continued to grow until the present-day, possibly related to down-dip gliding associated to updip extension. The diapirs, characterized by a relatively fine drape-folded roof, were not at this stage arranged in salt walls but rather as individual salt stocks. From this phase onwards (from the beginning of the Pliocene), concordant and non-concordant deformations in the transitional and oceanic crust domains, respectively, become more distinct. Nevertheless, no structural variation that could explain this salt deformation difference has been observed in the available data.

During phase 3 (Fig. 12d), concomitant with major sedimentary input from the Rhône River (Fig. 11B), salt is actively deforming in the transitional crustal domain (pillow-like structures) and in the oceanic domain (near-surface passive diapirism). The important Rhodanian sediment supply, especially when it doubled after 0.9 Ma, may have influenced the salt structures growing directions, probably orienting them in the present-day thalweg direction (N-S and NW-SE) (Inset bathymetry Fig. 6). We suggest that salt, hitherto organized in salt stocks, forms salt walls that follow the main directions of the Rhône thalwegs. A more in-depth analysis of the spatial and temporal evolution focused on salt stocks in the deep basin would be necessary to confirm the relationship with Rhône sedimentary input. During phase 3, listric faults in the Extensional domain are locally still active and thus deforming the seafloor.

The difference in salt deformation intensity and morphologies between the transitional and oceanic crust domains (Tab. 1) is hard to explain when considering conventional driving forces like sedimentary loading, gravity or tectonic influence. No remarkable post-Messinian sedimentary thickness difference is recorded between the two domains, nor any difference in base salt inclination that could have generated differences in the evolution of salt tectonics. A tectonic component is unlikely as a thick sedimentary blanket separates the basement from the salt deposits and no significant Oligocene-Miocene fault activity displacing the base salt is observed. The first hypothesis we consider plausible is a temperature difference given by the underlying crustal nature. The viscosity of the salt is directly related to temperature: at higher temperatures, its viscosity decreases, thus favoring its movement. Heat flow measurements in the Provençal Basin (Burrus and Foucher, 1986; Poort *et al.*, 2020) have shown a warmer proto-oceanic crust ($>100\,\text{mW/m}^2$) than transitional crust ($50–60\,\text{mW/m}^2$). This heat flow trend is not surprising considering the young age of the basin and is consistent with other world areas where a young oceanic crust shows high heat flow values. However, it is still unclear how temperature would influence the evolution of salt structures, which are characterized by a thermal conductivity two to three times

higher than the sediments they are surrounded by. Basal heat is channeled into the diapirs up to the surface. Thus, as the diapir grows, it channels additional heat from the crust, further decreasing the salt viscosity and enhancing its mobility. In addition, fluids are well known to transfer heat. Upper oceanic crust is more porous and permeable than the continental crust, allowing active fluid circulation to the sedimentary column, often associated with high heat flow (*e.g.* Bellucci *et al.*, 2024; Fisher and Becker, 2000). Although a thick sedimentary blanket above the basement, fluids could reach the sub-salt, generating overpressure (Dale *et al.*, 2021) and affecting the salt deformation history to some extent. These fluid leaks may also affect the composition of the salt layer and thus its rheology. Salt tectonics may not only be related to structural mechanisms but also to halite rheological response to temperature changes and fluid activity. Further heat flow measurements coupled with numerical models may elucidate part of these hypotheses.

7 Conclusions

The Provençal Basin proves to be a useful area in understanding salt tectonic mechanisms in a passive margin context. The structural and salt deformation characteristics differ substantially from the deposition and evolution of salt structures in other well-known salt passive margins. This work has established a detailed evolution of salt structures in space and time. The main conclusions are:

– The salt precipitated in the deep basin and lower slope: the initial salt thickness can be considered constant in the deep basin while it decreases at the basin edges, where it pinches out on pre-salt sediments. The salt was deposited long after the formation of the basin, in a tectonically stable context. The present-day variations in salt structures are therefore not structurally conditioned.

– The salt has been deforming since its deposition to the present-day, in a relatively short period (~5 Ma). Salt tectonics started very early, during the UU deposition (phase 1) and/or during the last phases of salt deposition. The Pliocene and Pleistocene salt movement can be divided into two more main phases (phases 2 and 3), resulting in morphologies distributed differently in space.

– The present-day salt walls direction in the deep basin were likely influenced by the dynamics of the Rhône sedimentary fan, strongly active since 0.9 Ma. Major sedimentary input could also explain the quiescence phase above the Transitional crust during phase 2 but hardly explain the intense and rapid deformation above the oceanic crust during this phase.

– Regardless the deformation phase, salt deformation appears to be more rapid and intense above the oceanic crust than in the continental or transitional crust domains. The salt deformation strain rate varies over time and space, showing an acceleration above the oceanic crust. We suggest that the salt morphologies – crustal segmentation relation could be explained by differences in temperature associated with different crustal natures. Salt above the oceanic crust, subject to higher temperature and/or potential water leaks associated with crustal nature that may impact the rheology and nature of the salt layer,

deforms more rapidly. This could explain the development of more evolved and discordant structures when compared to salt located above transitional crust.

Supplementary material

Supplementary Data 1. Velocities estimation for each reflector on the ESP positions. ESP velocities from Pascal *et al.*, 1993). Modified from Leroux, 2012.

Supplementary Data 2. Velocities curves extracted from wells data on the shelf (Mistral, Tramontane, Calmar, Rascasse) on the upper slope (Autan1), and on the middle slope (GLP2). Depth of each of our main stratigraphic marker has been superimposed on these curves to estimate a mean velocity value for each stratigraphic interval. Modified from Leroux, 2012.

The Supplementary Material is available at https://www.bsgf.fr/10.1051/bsgf/2024007/olm.

References

Afilhado A, Moulin M, Aslanian D, Schnürle P, Klingelhoefer F, Nouzé, H., Rabineau M *et al.* 2015. Deep crustal structure across a young passive margin from wide-angle and reflection seismic data (The SARDINIA Experiment)-II. Sardinia's margin. Bull. Soc. Géolog France 186: 331–351.

Auzende JM, Bonnin J, Olivet JL 1973. The origin of the western Mediterraneanbasin. J Geolog Soc 129:607–620.

Bache F, Olivet JL, Gorini C, Rabineau M, Baztan J, Aslanian D, Suc JP. 2009. Messinian erosional and salinity crises: view from the Provence Basin (Gulf of Lions, Western Mediterranean). Earth Planet Sci Lett 286: 139–157.

Bache F, Olivet JL, Gorini C, Aslanian D, Labails C, Rabineau M. 2010. Evolution of rifted continental margins: the case of the Gulf of Lions (Western Mediterranean Basin). Earth Planet Sci Lett 292: 345–356.

Bache F, Gargani J, Suc JP, Gorini C, Rabineau M, Popescu SM, Leroux E, Do Couto D, Jouannic G, Rubino J-L., Olivet J-L., Clauzon G, Dos Reis AT, Aslanian D. 2015. Messinian evaporite deposition during sea level rise in the Gulf of Lions (Western Mediterranean). Mar Petrol Geol 66: 262–277.

Badhani S, Cattaneo A, Dennielou B, Leroux E, Colin F, Thomas Y, Jouet G, Rabineau M, Droz L. 2020. Morphology of retrogressive failures in the Eastern Rhône interfluve during the last glacial maximum (Gulf of Lions, Western Mediterranean). Geomorphology 351: 106894.

Bassetti MA, Berne S, Jouet G, Taviani M, Dennielou B, Flores JA, Gaillot A, Gelfort R, Lafuerza S, Sultan N. 2008. The 100-ka and rapid sea level changes recorded by prograding shelf sand bodies in the Gulf of Lions (western Mediterranean Sea). Geochem Geophys Geosyst 9(11).

Benson RH, Rakic-El Bied K, Bonaduce G. 1991. An important current reversal (influx) in the Rifian Corridor (Morocco) at the Tortonian-Messinian boundary: The end of Tethys Ocean. Paleoceanography 6: 165–192.

Bellucci M. 2021. Relationship between crustal segmentation, nature, thermicity and salt tectonics in the Western Mediterranean Sea (Doctoral dissertation, Université de Bretagne occidentale-Brest; Università degli studi (Trieste, Italie)).

Bellucci M, Aslanian D, Moulin M, Rabineau M, Leroux E, Pellen R, Poort J, Del Ben A, Gorini C, Camerlenghi A. 2021a. Salt morphologies and crustal segmentation relationship: New insights from the Western Mediterranean Sea. Earth-Sci Rev 103818.

Bellucci M, Pellen R, Leroux E, Bache F, Garcia M, Do Couto D, Raad F, Blondel S, Rabineau M, Gorini C, Moulin M, Maillard A, Lofi J, Del Ben A, Camerlenghi A, Poort J, Aslanian D. 2021b. A comprehensive and updated compilation of the seismic stratigraphy markers in the Western Mediterranean Sea. SEANOE. https://doi.org/10.17882/80128.

Bellucci M, Poort J, Lucazeau F, Rolandone F, Do Couto D. *et al*. (2024). New heat flow data on the South Balearic margin: Evidence of regional fluid circulation system. Tectonophysics, 870, 230155.

Blondel S, Bellucci M, Evans S, Del Ben A, Camerlenghi A. 2022. Contractional salt deformation in a recently inverted basin: Miocene to current salt deformation within the central Algerian basin. Basin Research.

Brun JP, Fort X. 2011. Salt tectonics at passive margins: geology versus models. Mar Petrol Geol 28: 1123–1145.

Burrus J, Foucher JP. 1986. Contribution to the thermal regime of the Provençal Basin based on FLUMED heat flow surveys and previous investigations. Tectonophysics 128: 303–334.

Carter NL, Horseman ST, Russell JE, Handin J. 1993. Rheology of rocksalt. J Struct Geol 15: 1257–1271.

Christeleit EC, Brandon MT, Zhuang G. 2015. Evidence for deep-water deposition of abyssal Mediterranean evaporites during the Messinian salinity crisis. Earth Planet Sci Lett 427: 226–235.

CIESM. 2008. The Messinian salinity crisis from mega-deposits to microbiology. In: Briand, F. (Ed.), A consensus report, in 33'eme CIESM Workshop Monographs, 33. CIESM 16, bd de Suisse, MC-98000, Monaco, pp. 1–168.

Clauzon G. 1982. Le canyon messinien du Rhône; une preuve decive du" desiccated deep-basin model ». Bull Soc Géolog France 7: 597–610.

Clauzon G, Suc JP, Gautier F, Berger A, Loutre MF. 1996. Alternate interpretation of the Messinian salinity crisis: controversy resolved? Geology 24: 363–366.

Cobbold PR, Szatmari P. 1991. Radial gravitational gliding on passive margins. Tectonophysics 188: 249–289.

Dal Cin M, Del Ben A, Mocnik A, Accaino F, Geletti R, Wardell N, Zgur F, Camerlenghi A. 2016. Seismic imaging of Late Miocene (Messinian) evaporites from Western Mediterranean back-arc basins. Petrol Geosci 22: 297–308.

Dale MS, Marín-Moreno H, Falcon-Suarez IH, Grattoni C, Bull JM, McNeill LC. 2021. The Messinian Salinity Crisis as a trigger for high pore pressure development in the Western Mediterranean. Basin Res 33: 2202–2228.

Demercian S, Szatmari P, Cobbold PR. 1993. Style and pattern of salt diapirs due to thin skinned gravitational gliding, Campos and Santos basins, offshore Brazil. Tectonophysics 228: 393–433.

Dooley TP, Hudec MR, Carruthers D, Jackson MP, Luo G. 2017. The effects of base-salt relief on salt flow and suprasalt deformation patterns—Part 1: Flow across simple steps in the base of salt. Interpretation 5: SD1–SD23.

Dos Reis AT. 2001. La Tectonique Salifère et son Influence sur l'Architecture Sédimentaire Quaternaire de la Marge du Golfe du Lion- Méditérranée Occidentale (Doctoral dissertation). Université de Bretagne Occidentale.

Dos Reis AT, Gorini C, Mauffret A. 2005. Implications of salt-sediment interactions on the architecture of the Gulf of Lions deep-water sedimentary systems—western Mediterranean Sea. Mar Petrol Geol 22: 713–746.

Dos Reis AT, Gorini C, Weibull W, Perovano R, Mepen M, Ferreira É. 2008. Radial gravitacional gliding indicated by subsalt relief and salt-related structures: the example of the gulf of Lions, western Mediterranean. Rev Brasil Geofís 26: 347–365.

Droz L. 2003. PROGRES cruise, RV Le Suroît, https://doi.org/10.17600/3020080

Droz L, Jégou I, Gillet H, Dennielou B, Bez M, Canals M, Amblas D, Lastras G, Rabineau M. 2020. On the termination of deep-sea fan channels: Examples from the Rhône Fan (Gulf of Lion, Western Mediterranean Sea). Geomorphology 369: 107368.

Duffy OB, Hudec M, Peel F, Apps G, Bump A, Moscardelli L, Dooley T, Bhattacharya S, Wisian K, Shuster M. 2022. The role of salt tectonics in the energy transition: An overview and future challenges.

Duval B, Cramez C, Jackson MPA. 1992. Raft tectonics in the Kwanza basin, Angola. Mar Petrol Geol 9: 389–404.

Fisher AT, Becker K. 2000. Channelized fluid flow in oceanic crust reconciles heat-flow and permeability data. Nature 403: 71–74.

Gattacceca J, Deino A, Rizzo R, Jones DS, Henry B, Beaudoin B, Vadeboin F. 2007. Miocene rotation of Sardinia: new paleomagnetic and geochronological constraints and geodynamic implications. Earth Planet Sci Lett 258: 359–377.

Gaullier V. 1993. Diapirisme salifère et dynamique sédimentaire dans le bassin Liguro-Provençal. Données sismiques et modèles analogiques: Thèse, Université de Paris, 327.

Gaullier V, Loncke L, Vendeville B, Déverchère J, Droz L, Obone Zue Obane EM, Mascle J. 2008. Salt tectonics in the deep Mediterranean: indirect clues for understanding the Messinian Salinity Crisis. The Messinian salinity crisis from mega-deposits to microbiology-A consensus report, 91–96.

Gaullier, V., Chanier, F., Lymer, G., Vendeville, B. C., Maillard, A., Thinon, I. *et al*. (2014). Salt tectonics and crustal tectonics along the Eastern Sardinian margin, Western Tyrrhenian: New insights from the "METYSS 1" cruise. Tectonophysics, 615, 69–84.

Gaullier V, Vendeville B, Lofi J, Droz L, Sage F. 2018. Diachronous salt tectonics along the Gulf of Lions margin, Western Mediterranean. In EGU General Assembly Conference Abstracts (p. 17669).

Gautier F, Clauzon G, Suc J-P., Cravatte J, Violanti D. 1994. Age et durée de la crise de salinité messinienne. Comptes-Rendus de l'Académie des Sciences de Paris (2) 318: 1103–1109.

Geletti R, Zgur F, Del Ben A, Buriola F, Fais S, Fedi M, Forte E, Mocnik A, Paoletti V, Pipan M, Ramella R, Romeo R, Romi A. 2014. The Messinian Salinity Crisis: new seismic evidence in the West-Sardinian Margin and Eastern Sardo-Provençal Basin (West Mediterranean Sea). Mar Geol 351: 76–90.

Gorini C. 1993. Géodynamique d'une marge passive: le Golfe du Lion (Méditerranée occidentale) (Doctoral dissertation).

Gorini C, Montadert L, Rabineau M. 2015. New imaging of the salinity crisis: Dual Messinian lowstand megasequences recorded in the deep basin of both the eastern and western Mediterranean. Mar Petrol Geol 66: 278–294.

Granado P, Urgeles R, Sàbat F, Albert-Villanueva E, Roca E, Muñoz JA, Mazzucca N, Gambini R. 2016. Geodynamical framework and hydrocarbon plays of a salt giant: the NW Mediterranean Basin. Petroleum Geosci 22: 309–321.

Hsü KJ, Ryan WB, Cita MB. 1973. Late Miocene desiccation of the Mediterranean. Nature 242: 240–244.

Jackson MPA, Hudec MR. 2017. Salt Tectonics: Principles and Practice. Cambridge University Press.

Ings S, Beaumont C, Gemmer L. 2004. Numerical modeling of salt tectonics on passive continental margins: preliminary assessment of the effects of sediment loading, buoyancy, margin tilt, and isostasy, in *24th Annual GCSSEPM Foundation*, Bob F. Perkins Research Conference Proceedings (Vol. 36, p. 69).

Le Cann C. 1987. Le diapirisme dans le bassin Liguro-Provençal (Méditerranée occidentale) (Doctoral dissertation, Université de Bretagne occidentale).

Leroux E. 2012. Quantification des flux sédimentaires et de la subsidence du bassin Provençal (Doctoral dissertation, Université de Bretagne occidentale-Brest).

Leroux E, Rabineau M, Aslanian D, Granjeon D, Droz L, Gorini C. 2014. Stratigraphic simulations of the shelf of the Gulf of Lions: testing subsidence rates and sea-level curves during the Pliocene and Pleistocene. Terra Nova 26: 230–238.

Leroux E, Aslanian D, Rabineau M, Moulin M, Granjeon D, Gorini C, Droz L. 2015a. Sedimentary markers in the Provençal basin (Western Mediterranean): a window into deep geodynamic processes. Terra Nova 27: 122–129.

Leroux E, Rabineau M, Aslanian D, Gorini C, Bache F, Moulin M, Pellen R, Granjeon D, Rubino JL. 2015b. Post-rift evolution of the Gulf of Lion margin tested by stratigraphic modelling. Bull Soc Géolog France 186: 291–308.

Leroux E, Rabineau M, Aslanian D, Gorini C, Molliex S, Bache F, Robin C, Droz L, Moulin M, Poort J, Rubino JL, Suc JP. 2017. High-resolution evolution of terrigenous sediment yields in the Provence Basin during the last 6 Ma: relation with climate and tectonics. Basin Res 29: 305–339.

Leroux E, Aslanian D, Rabineau M, Gorini C, Rubino J-L., Poort J, Suc J-P., Bache F, Blanpied C, *et al.* 2019. Atlas of the stratigraphic markers in the western mediterranean with focus on the Messinian, Pliocene and Pleistocene of the Gulf of Lion. CGMW (Commision for the Geological Map of the World) editor,73p + CD. https://ccgm.org/fr/atlas/199-atlas-of-the-stratigraphic-markers-in-the-western-mediterranean-the-gulf-of-lion-9782917310380.html

Letouzey, Colletta B, Vially RA, Chermette JC. 1995. Evolution of salt-related structures in compressional settings.

Lofi J. 2002. La crise de salinité messinienne: conséquences directes et différées sur l'évolution sédimentaire de la marge du Golfe du Lion. Diss. Lille 1. www.theses.fr/2002LIL10034

Lofi J, Gorini C, Berné, S., Clauzon G, Dos Reis AT, Ryan WB, Steckler MS. 2005. Erosional processes and paleo-environmental changes in the Western Gulf of Lions (SW France) during the Messinian Salinity Crisis. Mar Geol 217: 1–30.

Lofi J, Déverchère J, Gaullier V, Gillet H, Gorini C, Guennoc P, Loncke L, Maillard A, Sage F, Thinon I. 2011. Seismic atlas of the "messinian salinity crisis" markers in the mediterranean and black seas. Commun Geol Map World Mem SoC Géol de France, Nouvelle Śer. 72.

Lofi J. 2018. Seismic Atlas of the Messinian Salinity Crisis markers in the Mediterranean Sea-Volume 2 (Vol. 181, pp. 1–72). Société Géologique de France.

Maillard A, Gaullier V, Vendeville BC, Odonne F. 2003. Influence of differential compaction above basement steps on salt tectonics in the Ligurian-Provençal Basin, northwest Mediterranean. Mar Petrol Geol 20: 13–27.

Maillard A, Jolivet L, Lofi J, Thinon I, Couëffé R, Canva A, Dofal A. 2020. Transfer zones and associated volcanic province in the eastern Valencia Basin: Evidence for a hot rifted margin? Mar Petrol Geol 119: 104419.

Meilijson A, Hilgen F, Sepúlveda J, Steinberg J, Fairbank V, Flecker R, Waldmann N, Spaulding S, Bialik O, Garrett Boudinot F, Illner P, Makovsky Y. 2019. Chronology with a pinch of salt: Integrated stratigraphy of Messinian evaporites in the deep Eastern Mediterranean reveals long-lasting halite deposition during Atlantic connectivity. Earth Sci Rev 194: 374–398.

Mello UT, Karner GD, Anderson RN. 1995. Role of salt in restraining the maturation of subsalt source rocks. Mar Petrol Geol 12: 697–716.

Mianaekere V, Adam J. 2020a. 'Halo-kinematic' sequence stratigraphic analysis adjacent to salt diapirs in the deepwater contractional province, Liguro-Provençal Basin, Western Mediterranean Sea. Mar Petrol Geol 115: 104258.

Mianaekere V, Adam J. 2020b. 'Halo-kinematic' sequence-stratigraphic analysis of minibasins in the deepwater contractional province of the Liguro-Provençal basin, Western Mediterranean. Mar Petrol Geol 116: 104307.

Moulin M, Klingelhoefer F, Afilhado A, Aslanian D, Schnurle P, Nouzé, H., Rabineau M, Beslier MO, Feld A. 2015. Deep crustal structure across a young passive margin from wide-angle and reflection seismic data (The SARDINIA Experiment)-I. Gulf of Lion's margin. Bull. Soc. Géolog France 186: 309–330.

Obone-Zue-Obame EM, Gaullier V, Sage F, Maillard A, Lofi J, Vendeville B, Thinon I, Rehault JP. 2011. The sedimentary markers of the Messinian salinity crisis and their relation with salt tectonics on the Provençal margin (western Mediterranean): results from the "MAURESC" cruise. Bull Soc Géolog France 182: 181–196.

Olivet JL. 1996. La cinématique de la plaque ibérique. Bulletin des centres de recherches exploration-production Elf-Aquitaine 20: 131–195.

Pascal GP, Mauffret A, Patriat P. 1993. The ocean-continent boundary in the Gulf of Lion from analysis of expanding spread profiles and gravity modelling. Geophys J Int 113: 701–726.

Pautot G, Le Cann C, Coutelle A, Mart Y. 1984. Morphology and extension of the evaporitic structures of the Liguro—Provençal Basin: New Sea-Beam data. Mar Geol 55: 387–409.

Pellen R, Aslanian D, Rabineau M, Suc JP, Gorini C, Leroux E, Blanpied C, Silenziario C, Popescu SM, Rubino JL. 2019. The Messinian Ebro River incision. Glob Planet Change 181: 102988.

Poort J, Lucazeau F, Le Gal V, Dal Cin M, Leroux E, Bouzid A, Rabineau M, Palomino D, Battani A, Akhmanov GG, Ferrante GM, Gafurova DR, Bachir, R. Si, Koptev A, Tremblin M, Bellucci M, Pellen R, Camerlenghi A, Migeon S, Alonso B, Ercilla G, Yelles-Chaouche AK, Khlystov OM, 2020. Heat flow in the Western Mediterranean: Thermal anomalies on the margins, the seafloor and the transfer zones. Mar Geol 419: 106064.

Rabineau M. 2001. Un modèle géométrique et stratigraphique des séquences de dépôts quaternaires sur la marge du Golfe du Lion: enregistrement des cycles climatiques de 100 000 ans (Doctoral dissertation, Université de Rennes1).

Rabineau M, Berné S, Aslanian D, Olivet J-L, Joseph P, Guillocheau F, Bourillet J-F, Ledrezen E, Granjeon D. 2005 : Sedimentary sequences in the Gulf of Lions : a record of 100,000 years climatic cycles, Marine and Petroleum Geology, 22, p. 775-804).

Rabineau M, Berné S, Olivet JL, Aslanian D, Guillocheau F, Joseph P. 2006. Paleo sea levels reconsidered from direct observation of paleoshoreline position during Glacial Maxima (for the last 500,000 yr) . JT Earth Planet Sci Lett 252: 119–137.

Rabineau M, Leroux E, Aslanian D, Bache F, Gorini C, Moulin M, Molliex S, Droz L, dos Reis AT, Rubino JL, Guillocheau F, Olivet JL. 2014. Quantifying subsidence and isostatic readjustment using sedimentary paleomarkers, example from the Gulf of Lion. Earth Planet Sci Lett 388: 353–366.

Réhault JP, Boillot G, Mauffret A. 1984. The western Mediterranean basin geological evolution. Mar Geol 55: 447–477.

Rowan MG, Giles KA. 2021. Passive versus active salt diapirism. AAPG Bull 105: 53–63.

Sierro FJ, Andersen N, Bassetti MA, Berné S., Canals M, Curtis JH, Dennielou B, Flore JA, Frigola J, Gonzales-Mora B, Grimalt JO, Hodell DA, Jouet G, Pérez-Folgado M, Schneider R. 2009. Phase relationship between sea level and abrupt climate change. Pleistocene Sci Rev 28: 2867–2881.

Soto, J. I., Déverchère, J., Hudec, M. R., Medaouri, M., Badji, R., Gaullier, V., & Leffondré, P. (2022). Crustal structures and salt tectonics on the margins of the western Algerian Basin (Mediterranean Region). Marine and Petroleum Geology, 144, 105820.

Suc J-P., Clauzon G, Bessedik M, Leroy S, Zheng Z, Drivaliari A, Roiron P, Ambert P, Martinell J, Domenech R, Matias I, Julia R, Anglada R. 1992. Neogene and Lower Pleistocene in Southern France and Northeastern Spain. Mediterranean environments and climate. Cah Micropaleontol 7: 165–186.

Vail PR, Mitchum RM, Todd RG, Widmier JM, Thompson S, Sangree JB, Bubb JN, Hatlelid WG. 1977. Seismic stratigraphy and global changes of sea-level. Seismic stratigraphy-applications to hydrocarbon exploration. Memoir 26. American Association of Petroleum Geologists, Tulsa.

Vendeville BC. 2005. Salt tectonics driven by sediment progradation: Part I—Mechanics and kinematics. AAPG Bull 89: 1071–1079.

Wessel P, Smith WHF, Scharroo R, Luis J, Wobbe F. 2019. The Generic Mapping Tools. GMT Man Pages. Release 5.4. 5. Computer software manual. USA-2019